SYNTHESIS OF BENZIMIDAZOLE CONTAINING DONOR ACCEPTOR ELECTROCHROMIC POLYMERS

A THESIS SUBMITTED TO
THE GRADUATE SCHOOL OF NATURAL AND APPLIED SCIENCES
OF
MIDDLE EAST TECHNICAL UNIVERSITY

BY

HAVA ZEKİYE AKPINAR

IN PARTIAL FULFILLMENT OF THE REQUIREMENTS
FOR
THE DEGREE OF MASTER OF SCIENCE
IN
CHEMISTRY

FEBRUARY 2011

Approval of the thesis:

SYNTHESIS OF BENZIMIDAZOLE CONTAINING DONOR ACCEPTOR ELECTROCHROMIC POLYMERS

submitted by **HAVA ZEKİYE AKPINAR** in partial fulfillment of the requirements for the degree of **Master of Science in Chemistry Department, Middle East Technical University** by,

Prof. Dr. Canan Özgen
Dean, Graduate School of **Natural and Applied Sciences** _____

Prof. Dr. İlker Özkan
Head of Department, **Chemistry** _____

Prof. Dr. Levent Toppare
Supervisor, **Chemistry Dept., METU** _____

Examining Committee Members:

Prof. Dr. Duygu Kısakürek
Chemistry Dept., METU _____

Prof. Dr. Savaş Küçükyavuz
Chemistry Dept., METU _____

Prof. Dr. Levent Toppare
Chemistry Dept., METU _____

Assoc. Dr. Yasemin Arslan Udum
Chemistry Dept., Gazi University _____

Assist. Prof. Dr. Ali Çırpan
Chemistry Dept., METU _____

Date:

I hereby declare that all information in this document has been obtained and presented in accordance with academic rules and ethical conduct. I also declare that, as required by these rules and conduct, I have fully cited and referenced all material and results that are not original to this work.

Name, Last name: HAVA ZEKİYE AKPINAR

Signature

ABSTRACT

SYNTHESIS OF BENZIMIDAZOLE CONTAINING DONOR ACCEPTOR ELECTROCHROMIC POLYMERS

Akpınar, Hava Zekiye

M. Sc., Department of Chemistry

Supervisor: Prof. Dr. Levent Toppare

February 2011, 60 pages

Donor-acceptor-donor (DAD) type benzimidazole (BIm) and 3,4-ethylenedioxythiophene (EDOT) bearing monomers (4-(2,3-Dihydrothieno[3,4-b][1,4]dioxin-5-yl)-7-(2,3 dihydrothieno[3,4b][1,4] dioxin-7-yl)-2-benzyl-1H-benzo[d]imidazole (**M1**), 2,4-bis(2,3-dihydrothieno[3,4-b][1,4]dioxin-5-yl)-7-(2,3-dihydrothieno[3,4-b][1,4]dioxin-7-yl)-1H-benzo[d]imidazole (**M2**) and 4-(2,3-dihydrothieno[3,4-b][1,4]dioxin-5-yl)-7-(2,3-dihydrothieno[3,4-b][1,4]dioxin-7-yl)-2-ferrocenyl-1H-benzo[d]imidazole (**M3**)) were synthesized and electrochemically polymerized. Pendant group at 2-C position of the imidazole ring was functionalized with phenyl (**P1**), EDOT (**P2**) and ferrocene (**P3**) in order to observe substituent effect on electrochemical and electrochromic properties of corresponding polymers. Spectroelectrochemical results showed that different pendant groups resulted in polymers with slightly different optical band gaps (1.75, 1.69 and 1.77 eV respectively) and different number of achievable colored states. Optoelectronic performance were reported in detail.

Keywords: Benzimidazole, EDOT, Donor-Acceptor Type Polymers, Electrochromism, Conjugated Polymers.

ÖZ

BENZİMİDAZOL İÇEREN DONÖR AKSEPTÖR GRUPLAR İÇEREN ELEKTROKROMİK POLİMERLERİN SENTEZİ

Akpınar, Hava Zekiye
Yüksek Lisans, Kimya Bölümü
Tez Yöneticisi: Prof. Dr. Levent Toppare

Şubat 2011, 60 sayfa

Donör-akseptör-donör (DAD) tipi benzimidazol (BIm) ve 3,4-ethylenedioxythiophene (EDOT) içeren monomerler (4-(2,3-Dihidrotieno[3,4-b][1,4]dioksin-5-yl)-7-(2,3-dihidrotieno[3,4b][1,4] dioksin-7-yl)-2-benzil-1H-benzo[d]imidazol (**M1**), 2,4-bis(2,3-dihidrotieno[3,4-b][1,4]dioksin-5-yl)-7-(2,3-dihidrotieno[3,4-b][1,4]dioksin-7-yl)-1H-benzo[d]imidazol (**M2**) and 4-(2,3-dihidrotieno[3,4-b][1,4]dioksin-5-yl)-7-(2,3-dihidrotieno[3,4-b][1,4]dioksin-7-yl)-2-ferrosenil-1H-benzo[d]imidazol (**M3**)) sentezlenmiş ve elektrokimyasal olarak polimerleştirilmiştir. Çeşitli grupların ilgili polimerlerin elektrokimyasal ve elektrokromik özelliklerine olan etkilerini inceleyebilmek için imidazol halkasının 2-C pozisyonuna bağlı grup fenil (P1), EDOT (P2) ve ferrosen (P3) olmak üzere türevlendirilmiştir. Elde edilen spektroelektrokimyasal sonuçlara göre, monomerlere bağlanan her farklı grubun ilgili polimerlerin optik band aralıklarına olan etkisinin az olduğu gözlemlenmiştir. Band aralıkları sırasıyla 1.75, 1.69 ve 1.77 eV olarak hesaplanmıştır. Polimerlerin optoelektronik özellikleri detaylı şekilde rapor edilmiştir.

Anahtar kelimeler: Benzimidazol, EDOT, Donör-Akseptör Tipi Polimerler, Elektrokromism, Konjüge Polimerler.

To My Family

ACKNOWLEDGEMENTS

I would like to express my sincere thanks to my supervisor Prof. Dr. Levent Toppare for their guidance, support, encouragement, patience, advice, criticism and for listening and helping me in many ways.

I would like to thank to Elif Köse Ünver and Simge Tarkuç for their endless helps besides their kind friendship.

I would like to thank to Abidin Balan and Derya Baran for their valuable discussions and friendship.

I would like thank to all Toppare Research Group members for their cooperation and their kind friendship.

Many thanks to Fulya, Gözde, Gönül, Seda, Sema, Doğukan, Başak and Çilem for always being there for me, for their true friendship.

Words fail to express my eternal gratitude to my family for believing in me and giving me endless support.

I would like to express my special thanks to Çağdaş Cengiz for his continuous love and patience, I always know that he is with me and he never leaves me alone.

TABLE OF CONTENTS

LIST OF TABLES

TABLES

LIST OF FIGURES

FIGURES

LIST OF ABBREVIATIONS

ACN	Acetonitrile
CP	Conducting Polymer
CV	Cyclic Voltammetry
DAD	Donor Acceptor Donor
DCM	Dichloromethane
EDOT	3,4-Ethylenedioxythiophene
E_g	Band Gap Energy
Fc	Ferrocenyl
HOMO	Highest Occupied Molecular Orbital
ITO	Indium Tin Oxide
LED	Light Emitting Diode
LUMO	Lowest Unoccupied Molecular Orbital
NMR	Nuclear Magnetic Resonance
P3AT	Poly(3-hexylthiophene)
PA	Polyacetylene
PANI	Polyaniline
PCz	Polycarbazole
PEDOT	Poly(3,4-Ethylenedioxythiophene)
PF	Polyfuran
PPP	Poly(p-phenylene)
PPy	Polypyrrole
PRODOT	Poly(propylenedioxythiophene)
PTh	Polythiophene
PTSA	P-toluene sulfonic acid
$TBAPF_6$	Tetrabutylammonium hexafluorophosphate
VB	Valence Band

CHAPTER 1

INTRODUCTION

1.1 Conducting Polymers

First conducting polymer (CP) was produced by Letheby in 1862; however, developments started in this area in 90s. Letheby oxidized aniline in dilute sulphuric acid and observed a thick layer of bluish-green film on a sheet of platinum electrode [1]. In 1977, Shirakawa et al. showed that a covalent organic polymer would behave as a metal. They investigated the simplest organic polymer, polyacetylene (PA), which was synthesized as a silvery thin film using 1000 times of Ziegler-Natta catalyst by mistake. He succeeded to synthesize both cis and trans forms of PA (Figure 1.1) which are semiconductors. Trans isomer is thermodynamically stable at room temperature.

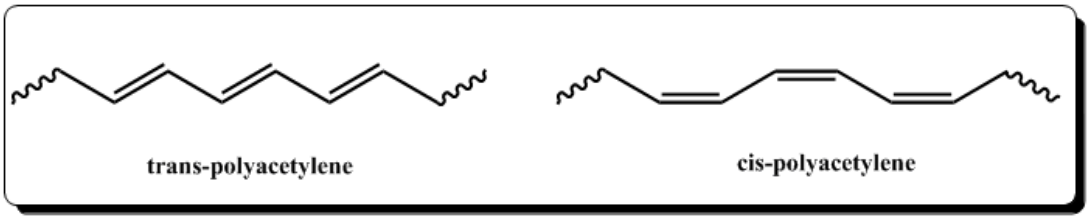

Figure 1. 1 Trans and cis forms of polyacetylene.

Then, they exposed these semiconductors to halogen vapour and measured their conductivities by four-probe dc techniques at room temperature. They observed that conductivity increases four and seven orders of magnitude of PA when it was exposed to strong electron acceptors, bromine and iodine vapours for several

minutes, respectively. These charge transfer π complexes, polyacetylene bromides and iodides, are formed during the halogenation of olefins. Polyacetylene halides are the first examples of organic polymers where electrical conductivity can be systematically varied over a range of eleven orders of magnitude by chemical doping [2,3].

In 2000, Hideki Shirakawa, Alan MacDiarmind and Alan Heeger were awarded with Chemistry Nobel Prize for their research in this area. Changing the hydrogen atoms with different organic and inorganic molecules created a new class of conducting polymers with different conductivities. Over the past 30 years, many types of conjugated polymers were synthesized containing different heterocyclics in their backbones such as pyrrole and thiophene [4-7]. (Figure 1.2)

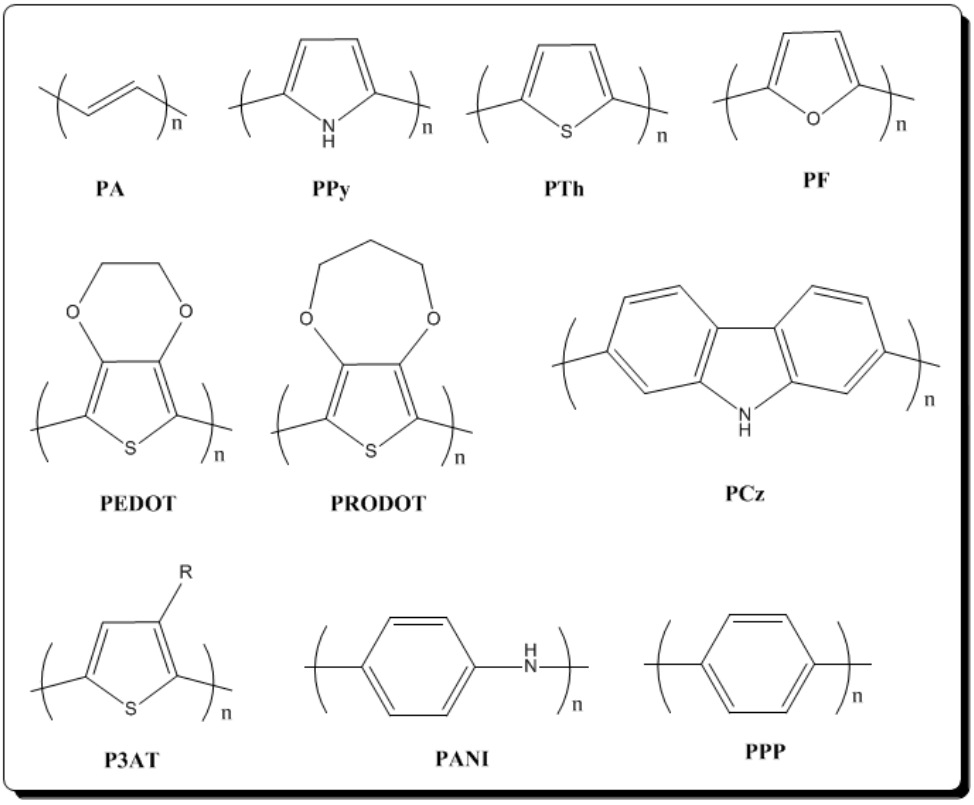

Figure 1. 2 Common organic conducting polymers.

The use of CPs as materials which possess the ability to change color reversibly by altering their redox state has a fast receiving attention. Overcoming the stability problem and the ability of modification of physical and optical properties of the electrically conducting, conjugated polymers allowed their use in many areas such as light-emitting displays [8], solar cells [9], electrochromic devices [10], and field-effect transistors [11].

1.2 Electrochemical Doping of Conjugated Polymers

Doping of conjugated polymers is a very important phenomenon since it affects greatly the optical properties as well as the mechanical properties of the desired polymers. The electronic structure of conjugated polymers can be varied by redox reactions. The concept of these redox reactions is similar with the doping of semiconducting inorganic materials. Basically, removing of an electron from the polymer chain is called p-doping and the addition of an electron into the polymer chain is called n-doping which enable the electrons to move freely through the backbone. In the literature, the number of p-doped conjugated polymers is higher than the n-doped ones since n-doping should be performed in compulsive conditions such as dry and oxygen free-medium. This difficulty is related to the instability of organic anions; these ions are easily oxidized with oxygen and water [12].

During oxidation reaction of a polymer, an electron is removed from the valence band, creates a hole in the structure which causes partial delocalization in the backbone. This p-doping process generates polaron and bipolaron bands. These new created energy levels lie between the HOMO and the LUMO levels of the polymer. Therefore, they allow lower energy transitions between these two states. As seen in Figure 1.3; polaron, radicalic cation, has a spin but bipolaron, dication, does not have a spin.

Conjugated polymers in their neutral states are composed of alternating single and double bonds through their polymer chains. When a polaron is created, the resulting chain absorbs in longer wavelengths than that of the neutral form. Created positive charge defect has a tendency to withdraw electrons from the lone pair of the heteroatom which generates quinoidal structure. These defects are stabilized by heteroatom and the aromatic stabilization energy. Removing the second electron from the same chain creates bipolaron which is stabilized by a second heteroatom for further stabilization. Therefore, bipolarons absorb radiation in longer wavelengths than that of the polaronic state. Most of the conjugated polymers synthesized so far are stable in their oxidized states and can be switched between their oxidized and neutral states many times.

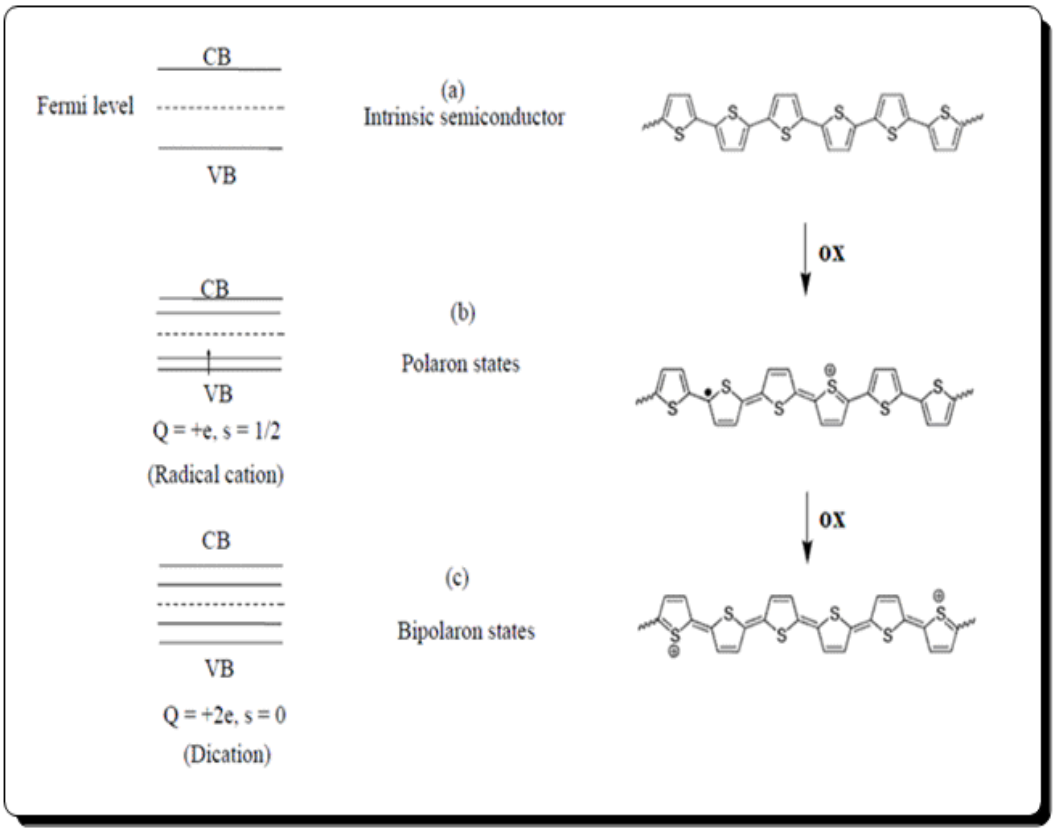

Figure 1. 3 Schematic representation of oxidized states of a polythiophene chain. a) Neutral polymer b) Polaron states c) Bipolaron states

1.3 Band Gap of Conjugated Polymers

Conjugated polymers are considered as semiconductors. Electrical behavior of semiconductors can be defined based upon band gap theory which is one of the most important characteristic in order to explain the optical properties of conjugated polymers. Basically, band gap is the energy gap between the two distinct energy levels; highest occupied state in valence band (VB) and the lowest unoccupied state in conduction band (CB). In semiconductors, this gap is small enough to transfer the free electrons from the HOMO level to the LUMO level at increased temperatures. In the doped semiconductors, the case is that there are new energy levels between the VB and the CB for electrons to reach to the conduction band. As seen in Figure 1.4, in conductors, these two bands are overlapped and in insulators, there is a large gap between them.

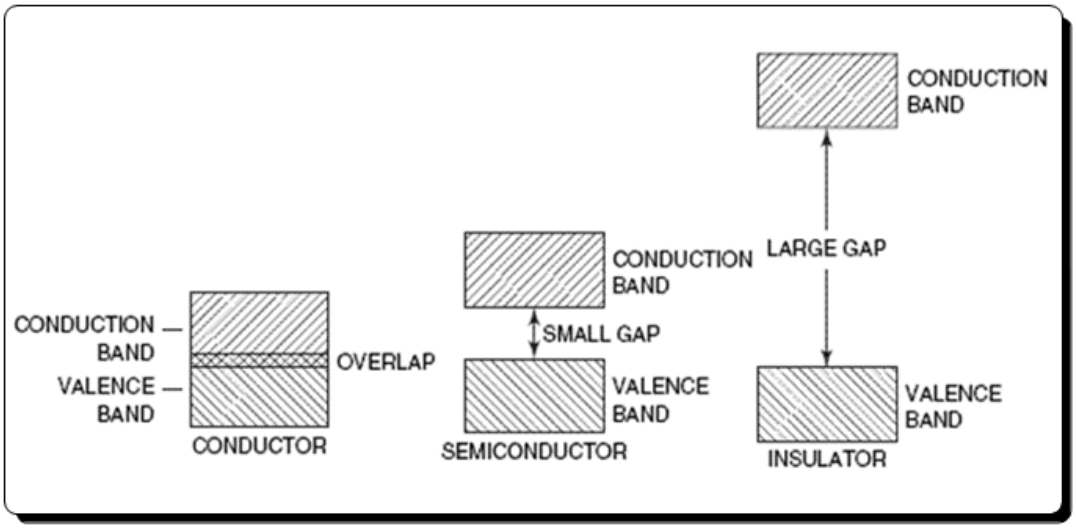

Figure 1. 4 Valence and conduction bands in conductor, semiconductor, and insulator.

This energy difference between two levels can be calculated from the onset of the highest wavelength absorption of a neutral polymer from a UV-Vis spectrum. Starting edge of this absorption peak is associated with the first π-π^* transition in the

polymer, minimum energy difference from the valence band to the conduction band. Therefore λ_{max} is reported according to this onset point in the spectrum, which is the term used to calculate the width of this energy gap [Eg (eV) = 1241/ λ_{max} (nm)]. Band gap can also be calculated by taking the difference between the onset points of oxidation and the reduction peaks of the polymer obtained from cyclic voltammetry (CV) if the polymer is n-dopable.

The factors affecting the band gap are planarity, resonance energy of the polymer backbone, inductive effects of the substituent, bond length alternation, and the interchain coupling in the solid state [13]. Considering the effects of these parameters, researchers synthesized various types of polymers and proved that this energy gap can be tuneable [14].

There are several methods in the literature that are used to lower the band gap of polymers. For instance, resonance affects the whole polymer backbone. Polyisonaphthene is a good example for this concept. Fused benzene ring to thiophene resulted in favored quinoid form of its polymer with 1,0 eV band gap energy where the band gap of polythiophene 2,2 eV without changing its aromaticity (Figure 1.5) [15].

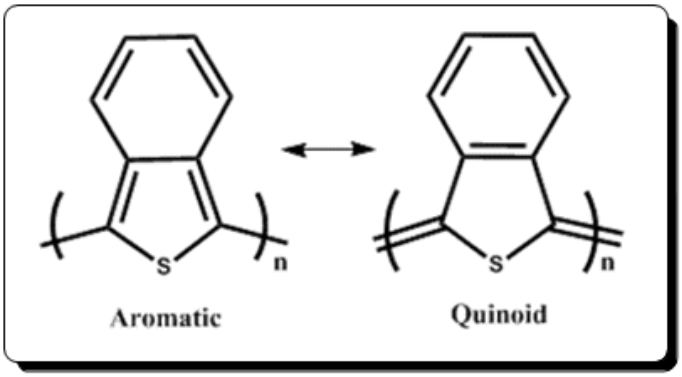

Figure 1. 5 Aromatic and quinoid states of polyisonaphthene.

Attenuating the impact of steric interactions between the repeating rings by placing spacer units into the chain is also a way for lowering the band gap. Donor-acceptor theory is the mostly used one for this purpose, modifying the structure as donor and acceptor sequentially leads to faster internal charge transfer and low band gap.

1.4 Low Band Gap Polymers

Band gap value is extremely important for conjugated polymers since it is directly related with the electron or hole affinities, absorption values and conductivities of polymers. Polymers having band gap value lower than 1,8 eV were classified as the low band gap materials. Synthesized conjugated polymers up to now have different band gap values. Low band gap polymers have gained a great deal of attention since they have many applications. For example, presence of a transmissive oxidized state of a material enables their use in smart window applications and light emitting displays. Small band gap polymers are also expected to have n-doping property which allows their usage in energy storage applications. Therefore, it is important to understand the factors which affect the band gap value of conjugated polymers.

Factors affecting the band gap value can be classified as following figure.

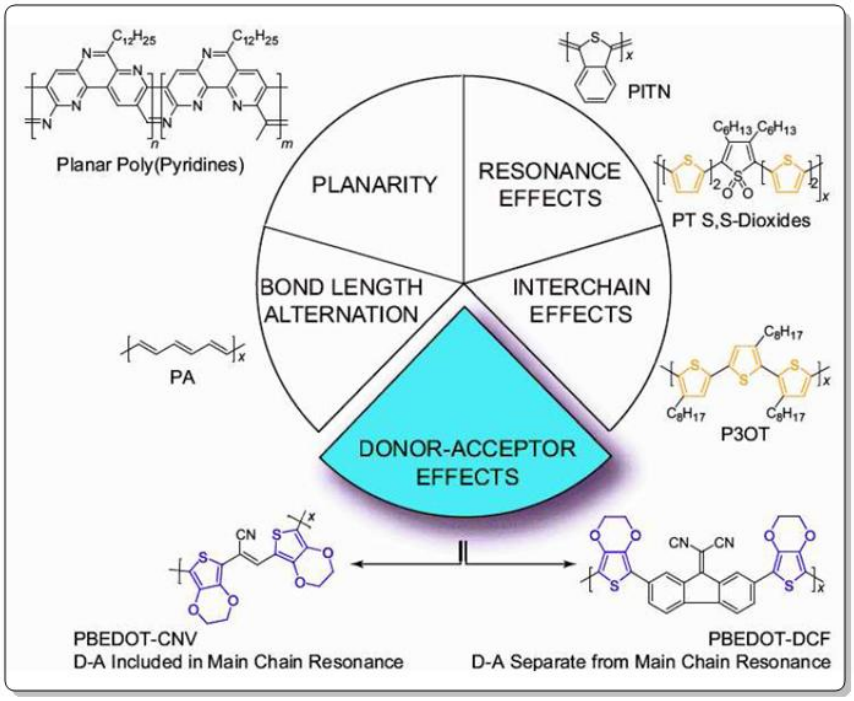

Figure 1. 6 Methods for the modification of band gap.

As indicated in Figure 1.6; planarity, resonance effects, interchain effects, bond length alternation and donor-acceptor approach are the factors which directly affect the band gap value. In order to get reduced band gap values, planarity of the molecular structure can be increased or donor- acceptor approach can be used which is the mostly used technique. In this theory, introducing a donor unit to an acceptor unit increases the π character of double bonds between the aromatic units on the polymer chains which results with a reduced band gap.

1.5 Donor-Acceptor Theory

Donor-acceptor theory is based on the attachment of one donor unit to an acceptor unit. This process causes lower band gap and wider band-width than either of the polymers of both units due to resonances [16]. One of the most important contributions of this theory is that the monomer structure can be modified. This

allows researchers to control the magnitude of the band gap via having the ability to choose different donor and acceptor units considering its electron donating and withdrawing strengths. More specifically, hybridization between the highest state of the HOMO level of the donor with the lowest state of the LUMO level of the acceptor leads to the polymer which has an ionization potential closer to donor and an electron affinity closer to the acceptor (Figure 1.7) [17].

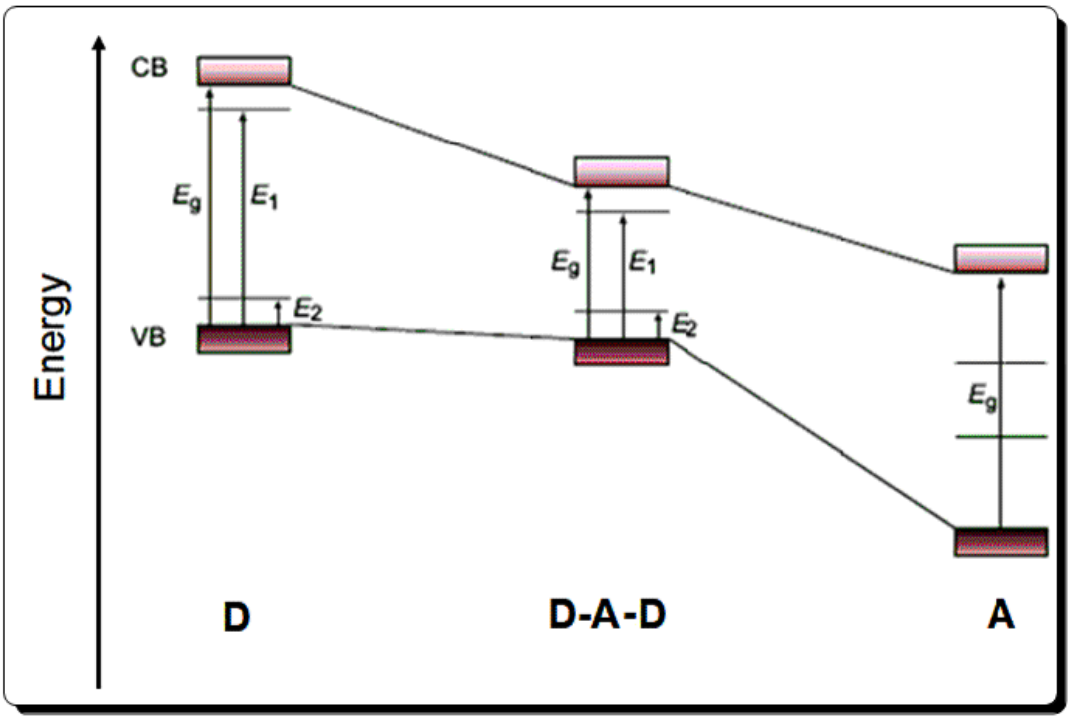

Figure 1. 7 Donor (D) -Acceptor (A) Concept.

1.6 Electrochromism

Electrochromism is basically defined as spectral change in a material when an external voltage is applied. Electroactive materials can gain electrons (reduction) or lose electrons (oxidation). During these electron transfers, different redox states are formed. Each of these states needs different energies to promote an electron between its ground state and its excited state which resulted as the generation of new bands in

the spectrum. This new bands may be formed in near IR region besides the VIS region. Therefore, in the characterization of electrochromic materials, CV and spectroscopic techniques are commonly employed where the π-π^* transitions, band gap, and the generation of new charge carriers in the polymer backbone under potentiostatic control can be determined.

Many inorganic and organic species possess electrochromic behavior such as viologens and metal oxides. Tungsten trioxide is the first example which shows color change by electrochemical reduction in 1930 [18]. Over the past two decades, electrochromic properties of conjugated polymers were examined. In conjugated polymers, these spectral changes become reversible due to its prolonged delocalization of the π-electrons along the conjugated backbone.

One of the major benefits of CP's is the ability to improve their electrochemical properties by structural modifications (Figure 1.8) [19]. Use of this benefit leads low oxidation potentials for monomers and fast switching times and a low band gap for the resulting polymer. In order to get such good electrochemical properties, there are several methods in designing the monomers. One of them is donor- acceptor theory. With the help of this theory, there are several examples in the literature showing good electrochemical properties [20-27].

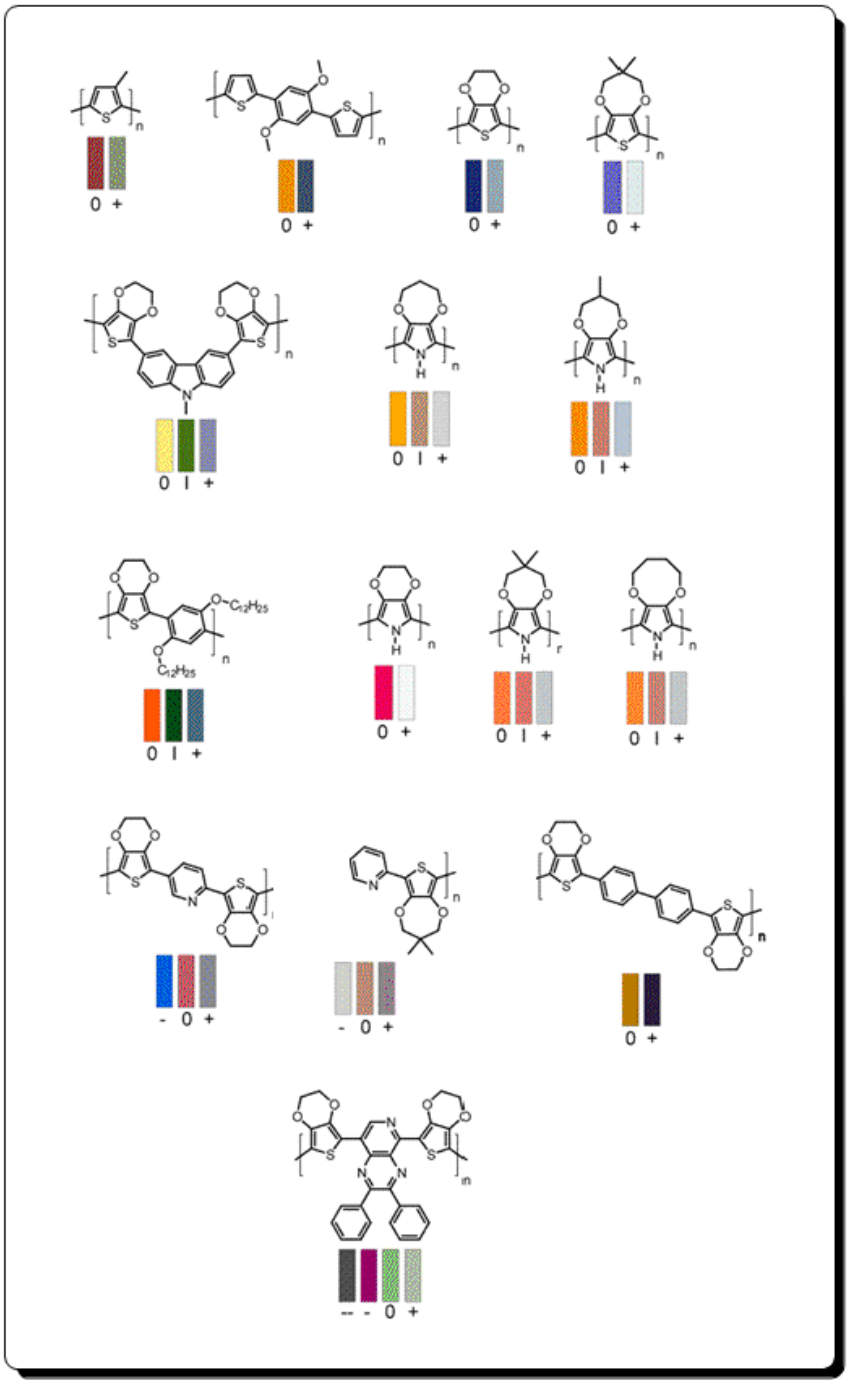

Figure 1. 8 Examples of multicolor electrochromic polymers synthesized by structural modification. 0 = neutral; I= intermediate; + =oxidized; and-- = reduced [19]

1.7 Pendant Group Effects

The electrochromic properties of conducting polymers can be improved by molecular modifications. After modification of the monomer structure, it must preserve its conjugated system. Pendant groups of the monomers do not participate in polymerization. Therefore, they do not have a major effect on the electronic structures of the resulting polymers. Structural effects of substitution such as inductive, mesomeric and steric were widely studied up to now [28]. Pendant groups affect the resulting polymers with different aspects such as reactivity of monomer, planarity of conjugated systems, morphology of the polymer film, and propagation of polymerization. Due to these reasons, the all the desired polymers can be obtained as electrochemical properties.

Substitution of a strong electron withdrawing group to the monomers resulted with higher oxidation potentials than the unsubstituted ones. For example 3-cyanothiophene and 3-nitrothiophene have oxidation potentials higher than thiophene itself [29]. This is because of the high reactivity of the radicals which have tendency to react with solvent or anions instead of initiating the polymerization [30]. On the other hand, substitution of a strong donor unit to the monomer decreases the oxidation potential of the monomer which means formed radicals are stable which favors the polymerization.

Mao Li and co-workers studied the substitution effects of alkyl chains on electrochromic behaviours of poly(alkyl-3,4-ethylenedioxyselenophene) (Figure 1.9).

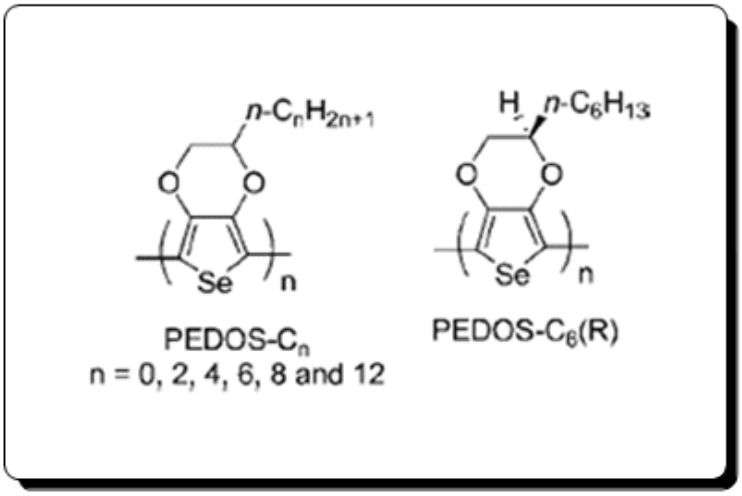

Figure 1. 9 PEDOS-C_n, *n* = 0, 2, 4, 6, 8 and 12 and PEDOS-C_6(R)

Results showed that electrochromic properties improve with PEDOS – C_6 (R), other derivaties have poorer properties in optical contrast, coloration efficiency and switching times. Long alkyl chains separate the polymer backbones from each other. The distance between the backbones causes faster doping process and easy transfer of counter ions within the film which enhances the switching time. Alkyl chains also increase the solubility of resulting polymers which is an important property in their applications [31].

Recently, pendant group effect of ferrocene unit on electrochromic characteristics was studied [32]. The outcome of the study indicated that multicolered states can be achieved with ferrocene unit since ferrocene has an individual electrochromic switch itself (Figure 1.10).

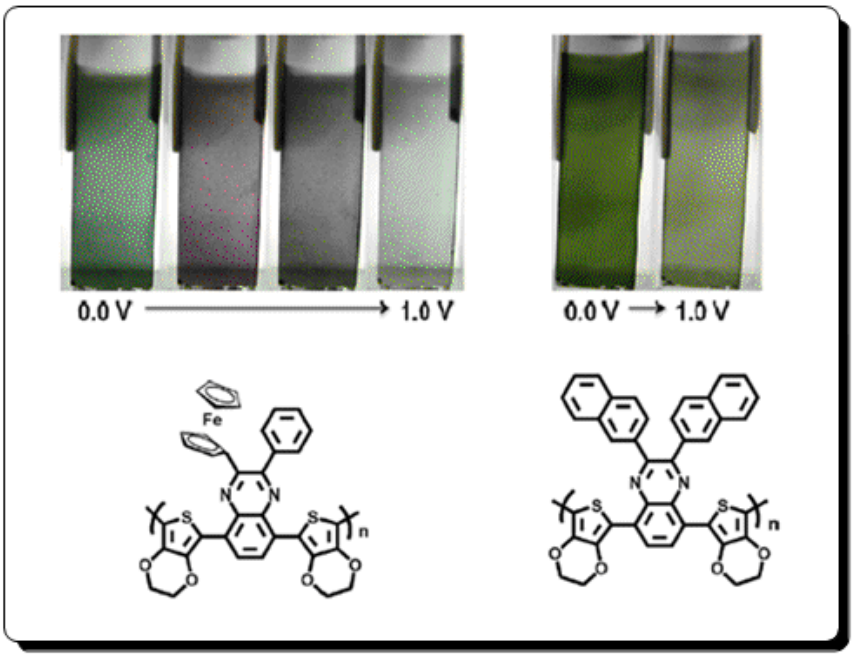

Figure 1. 10 Structures and colors of poly(5,8-bis(2,3-dihydrothieno[3,4 b][1,4]dioxin-5-yl)-2-(phenyll)-3-ferrocenylquinoxaline) and poly(5,8-bis(2,3-dihydrothieno[3,4-b][1,4]dioxin-5-yl)-2,3-di(naphthalen-2-yl)quinoxaline) [32].

1.8 Ferrocene

Ferrocene, with the molecular formula (Fe $(C_5H_5)_2$), is an electron-rich organometallic compound consisting of two cyclopentadienyl rings bound on opposite sides of a central iron atom (Figure 1.11). The reasons why ferrocene is preferred for functionalization of polymers are its electron rich character, its stability in both Fe(II) and Fe(III) oxidation states, steric effects and its easy substitution among a variety of functional groups [33].

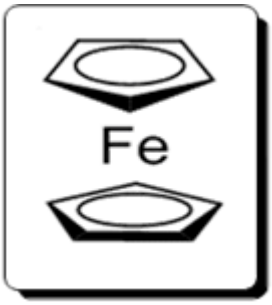

Figure 1. 11 Ferrocene.

By introducing a redox center into a polymer chain, the optical properties and the conductivity of the conjugated polymers can be adjusted. Therefore, inclusion of ferrocene, which shows good electron transfer properties, to polymer chains gained a lot of attention. Metal containing conducting polymers can be classified in three parts namely tethered (Type I), coupled (Type II) and incorporated (Type III) (Figure 1.12) [34].

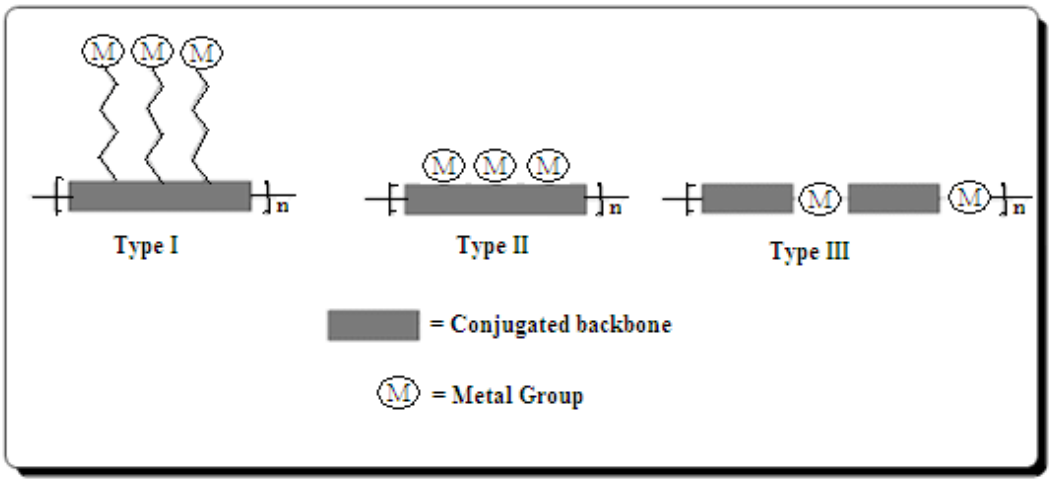

Figure 1. 12 Types of metal containing conducting polymers.

In the literature, ferrocene is a widely used compound in biosensor applications as electron transfer mediator between the enzyme and the electrode surface. In order to

prevent the leaking of the mediator, which causes sensor deactivation, mediator is linked to the enzyme or the polymer which resulted in the enhancement of the signal [35].

In order to observe the interactions between the electronic states of both polymer and a redox center, several ferrocene substituted polypyroles and polythiophenes were synthesized (Figure 1.13). These studies showed that insertion of ferrocene into a polyconjugated chain increases the conductivity of the chain [36].

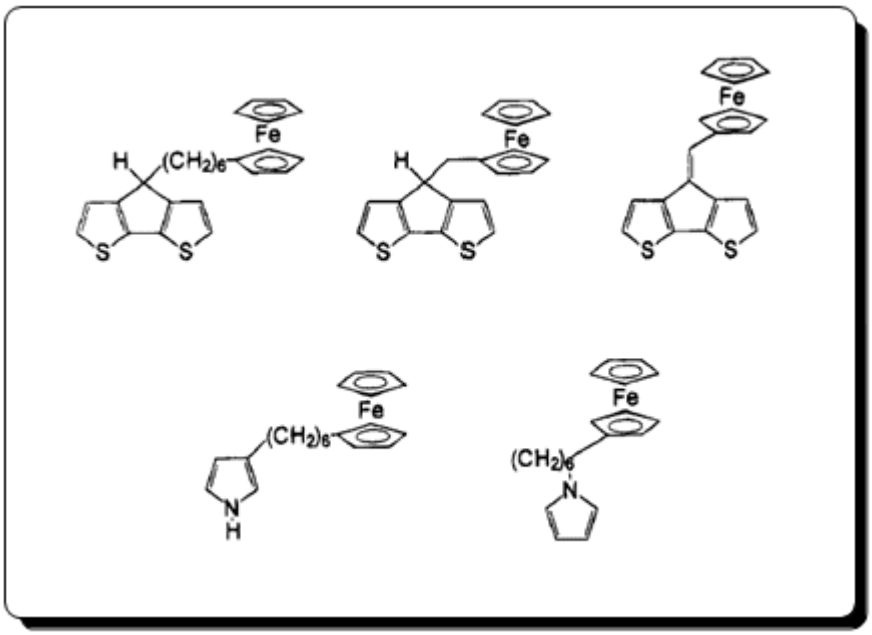

Figure 1. 13 Ferrocene substituted monomers.

Examples include ferrocene molecules which were directly inserted into a polymer chain are also available in the literature [37]. Studies showed that the stability of both Fe(II) and Fe(III) oxidation states of ferrocene makes the electropolymerization of oligothienylferrocene complexes without decomposition easier. Also, oxidation of the ferrocene group results in the formation of a low-energy charge transfer transition during electropolymerization.

1.9 Thiophene Based Conducting Polymers

Thiophene based molecules, rich in electron, are great candidates to be used as donor units in the monomers obeying DAD theory. Substitution of donor units to the β-positions of thiophene unit resulted with low monomer oxidation potential which prevents the overoxidation of polythiophene ring. In 1992, Gerhard Heywang and Friedrich Jonas showed that substitution of ethylenedioxy group into thiophene unit resulted with higher stability than polythiophene (PTh) [38]. Beside higher stability of this polymer, it was also proven to be an admirable choice for electrochromic devices due to its explicit advantages such as high optical contrast in the visible region, and fast switching time. PEDOT has ability to cycle between blue in the reduced state and a transmissive sky blue in the oxidized state (Figure 1.14) which is also a useful property for device applications [39].

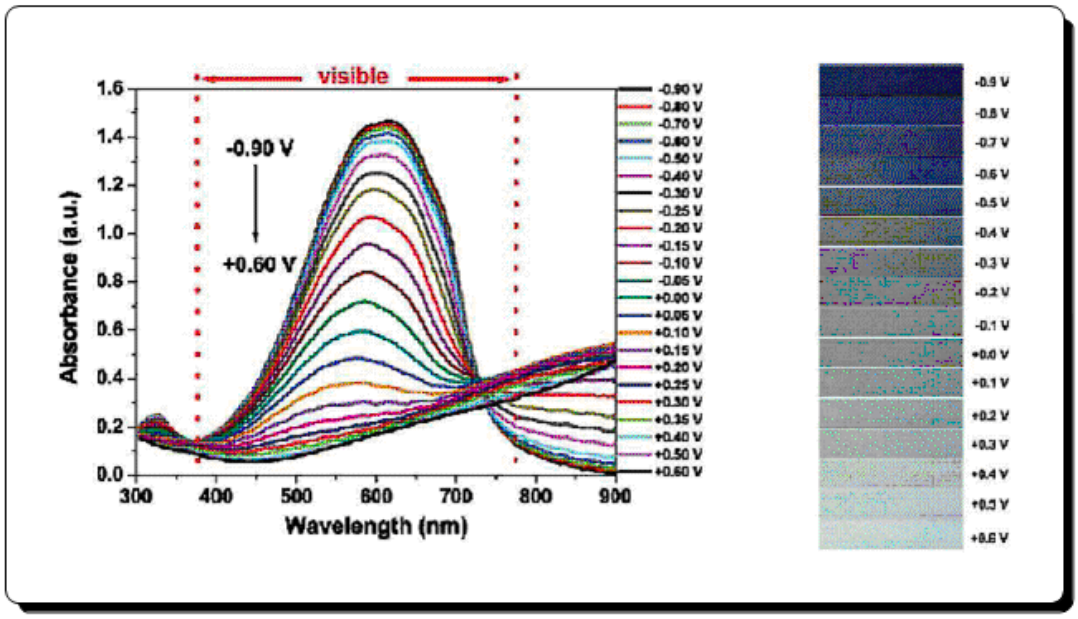

Figure 1. 14 Absorbance change during stepwise oxidation of PEDOT.

Electrochemical polymerization mechanism of EDOT is very similar to that of polythiophene (Figure 1.15).

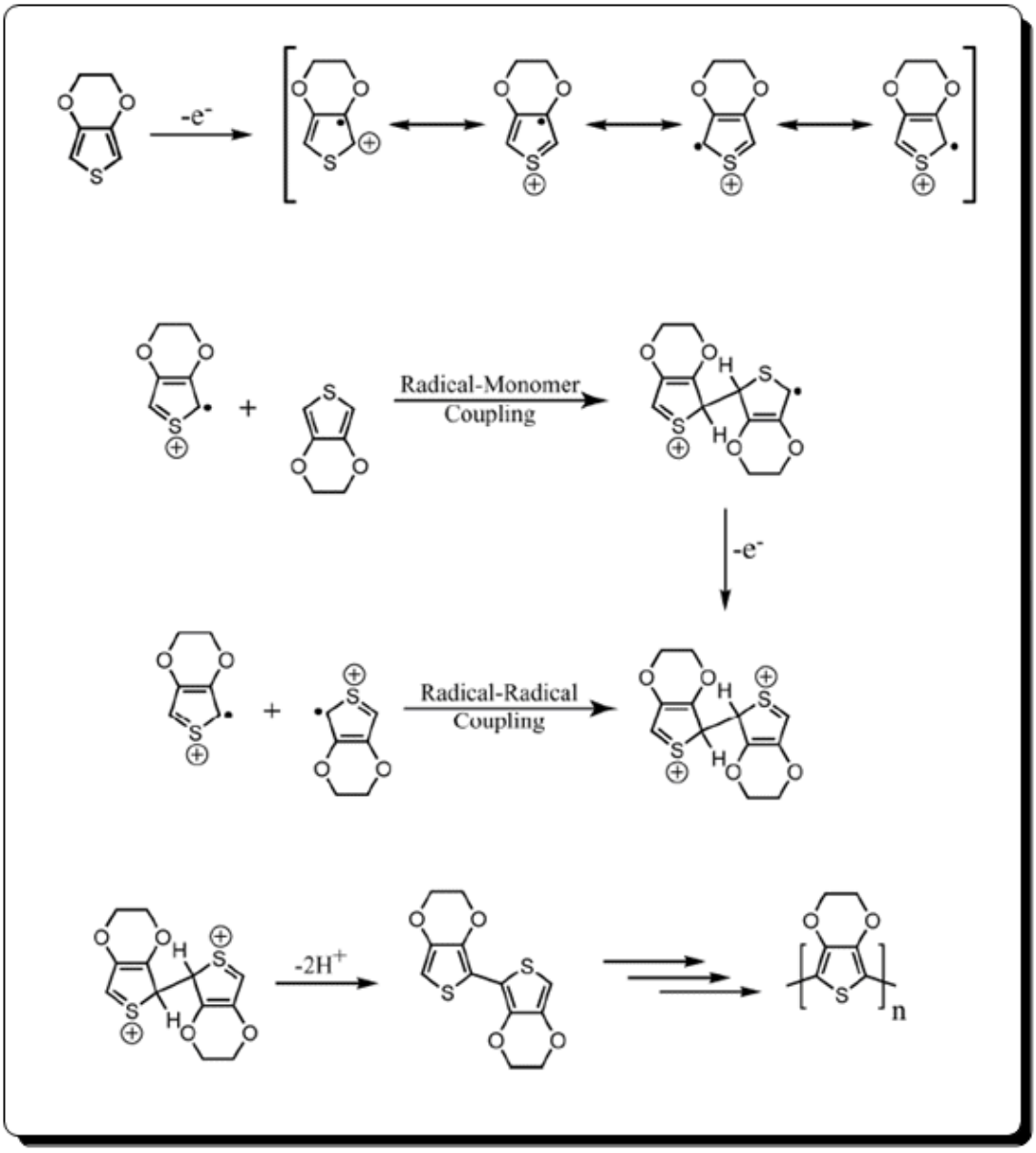

Figure 1. 15 Electrochemical polymerization mechanism of EDOT.

Presence of oxygen atoms causes PEDOT to have higher electron density than PTh. Therefore, PEDOT has higher HOMO level than PTh. Moreover, EDOT based molecules have lower oxidation potentials than their thiophene counterparts. In 2004,

donor acceptor donor types conjugated polymers with different donor units and with cyanovinylene as the acceptor unit were synthesized and their band gap values were calculated. Results showed that increasing the number of EDOT units in the backbone decreases the band gap value [40] (Figure 1.16).

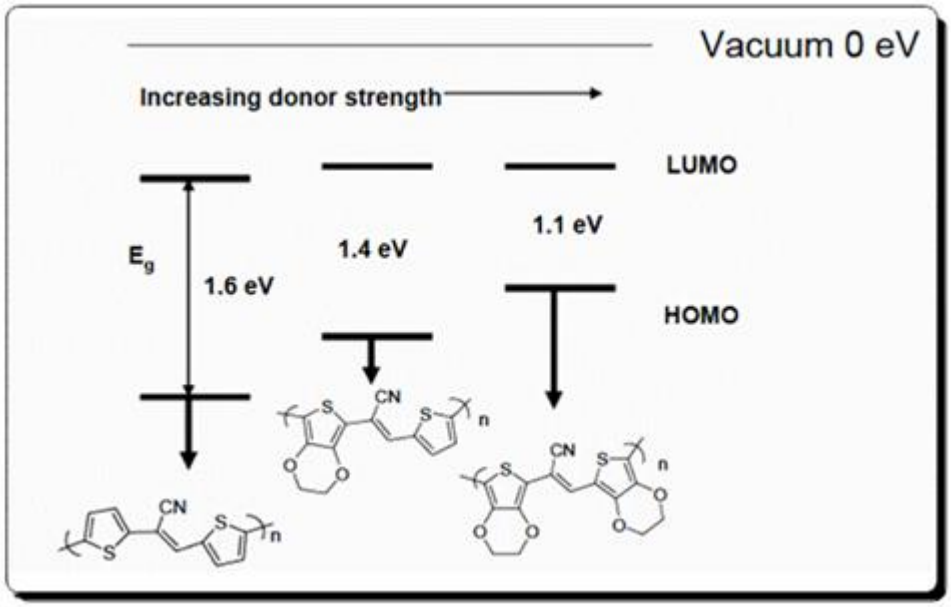

Figure 1. 16 Effect of donor unit on band gap.

1.10 Benzimidazole

Benzimidazole (BIm) is an aromatic organic compound which is a benzazole derivative. Benzothiadiazole (BTd), benzoselenadiazole (BSe), benzotriazole (BTz) are the other examples of benzazoles which were widely studied in electrochromism. Benzimidazole consists of the fusion of two cyclic compounds, benzene and imidazole (Figure 1.17).

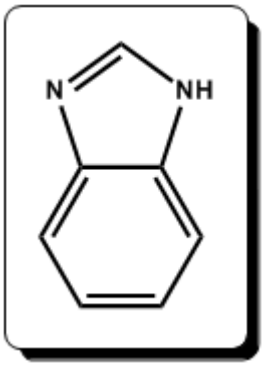

Figure 1. 17 Benzimidazole.

Containing conjugated π-bonds in its structure makes it an important candidate in order to synthesize conducting polymers. It is a biologically important compound which is found in Vitamin B12 and shows antitumor, antibacterial, and virucidal properties [41, 42]. In addition, chemically synthesized polybenzimidazoles showed great thermal stability and resistance at elevated temperatures [43]. Because of these unique properties, they have been widely used in the literature in biological applications and in the aerospace field [44-46].

On the other hand, sulfopropylated polybenzimidazole which is a proton conducting polymer was synthesized via ring opening reaction of 1,3-propanesultone on the reactive N-H groups of polybenzimidazole. Results showed that it has superior properties than those of conventional ion conducting polymers such as Nafion which is widely used in polymer electrolyte fuel cells [47]. Its first electropolymerization was performed by Shaheen Taj and co-workers in 2000 on a Pt electrode using acetonitrile containing 0,1 M $NaClO_4$. They proved that polymerization of benzimidazole and substituted benzimidazoles produce electroactive and conducting polymers [48].

Previously reported DAD type polymers obtained by coupling benzazoles with electron donating EDOT resulted in fine tuned electrochromic properties. BTd derivative DAD polymer was synthesized [49] and later it was shown to be the first

green to transmissive electrochromic polymer. BSe based polymer was also investigated as a green to transmissive polymer with red shifted absorptions compared to BTd derivative [51]. Recently, introduction of BTz units on PEDOT resulted in the enhancement of electrochromic properties such as optical contrast, switching time and coloration efficiency compare to parent polymer PEDOT [52]. Although, BTd, BSe and BTz based polymers and their different copolymers have been studied extensively in literature, DAD type electrochromic polymers with BIm as the acceptor unit are still unexplored up to date.

1.11 Aim of This Work

In this study, the syntheses and optoelectronic properties of BIm based DAD type polymers containing EDOT as the donor unit are highlighted. Substituent effect on electrochemical and optical properties was investigated. Substitution of benzene and EDOT units on 2-C position of BIm resulted in two homologue polymers. Additionally, ferrocene incorporation as pendant group was expected to reveal different redox behaviors due to its reversible and well defined electrochemical signal.

CHAPTER 2

EXPERIMENTAL

2.1 Materials and Methods

All chemicals were purchased from commercial sources and used without further purification. All reactions were carried out under argon atmosphere unless otherwise mentioned. 2,1,3-Benzothiadiazole (Aldrich), bromine (Br_2) (Merck), hydrobromic acid (HBr, 47%) (Merck), sodium borohydride ($NaBH_4$) (Merck), 3,4-ethylenedioxythiophene (EDOT) (Aldrich), ferrocene carboxaldehyde (Aldrich), benzaldehyde (Merck), *p*-toluenesulfonic acid (PTSA) (Aldrich), methanol (MeOH) (Aldrich), ethanol (EtOH) (Aldrich), hexane (C_6H_{14}) (Aldrich), ethylacetate (EtOAc) (Aldrich), chloroform ($CHCl_3$) (Aldrich), dichloromethane (DCM) (Aldrich), n-butyllithium (n-BuLi, 2.5M in hexane) (Acros Organics), tributyltin chloride ($Sn(Bu)_3Cl$, 96%) (Aldrich) were used as received. 4,7-Dibromobenzothiadiazole [53], 3,6-dibromobenzene-1,2-diamine [54], tributyl(2,3-dihydrothieno[3,4-b][1,4]dioxin-7-yl)stannane [55], 2,3-dihydrothieno[3,4 b][1,4]dioxine-5-carbaldehyde [56], 4,7-dibromo-2-phenyl-1H-benzo[d]imidazole [57] and 4,7-dibromo-2-(2,3-dihydrothieno[3,4-b][1,4]dioxin-5-yl)-1H-benzo [d]imidazole [57] were synthesized according to previously published procedures. Tetrahydrofuran (THF) (Fisher) was dried with benzophenon (Merck) and sodium prior to use.

2.2 Equipment

Electrochemical studies were performed in a three-electrode cell consisting of an Indium Tin Oxide doped glass slide (ITO) as the working electrode, platinum wire as

the counter electrode, and Ag wire as the pseudo reference electrode under ambient conditions using a Voltalab 50 potentiostat. ^{1}H and ^{13}C NMR spectra were recorded in $CDCl_3$ on Bruker Spectrospin Avance DPX-400 Spectrometer. Chemical shifts were given in ppm downfield from tetramethylsilane. Varian Cary 5000 UV-Vis spectrophotometer was used to perform the spectroelectrochemical studies of polymers. Mass analysis was carried out on a Bruker time-of flight (TOF) mass spectrometer with an electron impact ionization source.

2.3 Procedure, Synthesis

2.3.1 Synthesis of 4,7-dibromobenzothiadiazole (2)

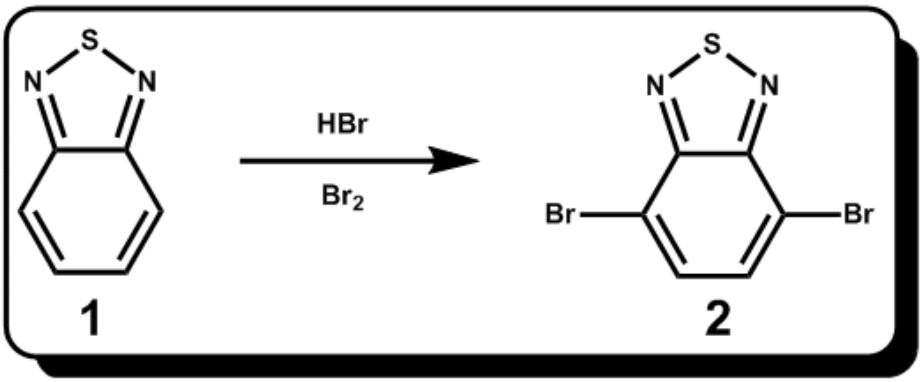

Figure 2. 1 Synthetic route for 4,7-dibromobenzothiadiazole (**2**).

4,7-Dibromobenzothiadiazole was synthesized according to the literature [53]. Benzothiadiazole (2.0 g, 14.69 mmol) was dissolved in HBr (36 mL) in a round bottom flask and fixed with a condenser. The mixed solution of Br_2 (1.6 mL) and HBr (16 mL) was added drop-wise to the mixture. After Br_2 addition was completed, the mixture was left to reflux for 6 h and cooled to room temperature. Precipitate was filtered and washed with saturated solution of $NaHSO_3$ in order to remove excess bromine. Precipitate was dissolved in DCM and extracted with water several times. Organic layer was dried over $MgSO_4$ and solvent was removed under vacuum and the crude product was obtained as a yellow solid in yield 90% (3.9 g, 13.22 mmol).

^{1}H NMR (400 MHz, $CDCl_3$) δ 7.66 (s, 2H). ^{13}C NMR (101 MHz, $CDCl_3$) δ 152.9, 132.3, 113.9.

2.3.2 Synthesis of 3,6-dibromobenzene-1,2-diamine (3)

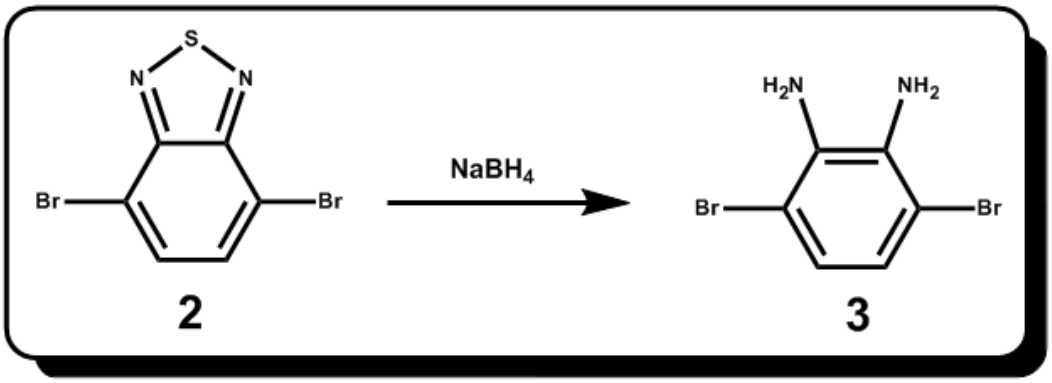

Figure 2. 2 Synthetic route for 3,6-dibromobenzene-1,2-diamine (**3**).

3,6-Dibromobenzene-1,2-diamine was synthesized according to the literature [54]. 4,7-Dibromobenzothiadiazole (**2**) (5,1 g, 17.35 mmol) was dissolved in EtOH (170 ml). $NaBH_4$ (12.2 g, 0.32 mol) was added slowly to the mixture during 4 h at 0 ^{o}C. After addition was completed, the mixture was stirred for 12 h at room temperature. EtOH was removed and crude product was dissolved in diethylether. Solution was extracted with brine. Organic layer was dried over $MgSO_4$ and the solvent was removed under vacuum and the crude product was obtained as a pale yellow solid in yield 87% (4.0 g, 15.09 mmol). ^{1}H NMR (400 MHz, $CDCl_3$) δ 6.78 (s, 2H), 3.82 (s, 4H). ^{13}C NMR (101 MHz, $CDCl_3$) δ 133.5, 123.2, 109.5.

2.3.3 Synthesis of 4,7-dibromo-2-phenyl-1H-benzo[d]imidazole (3a)

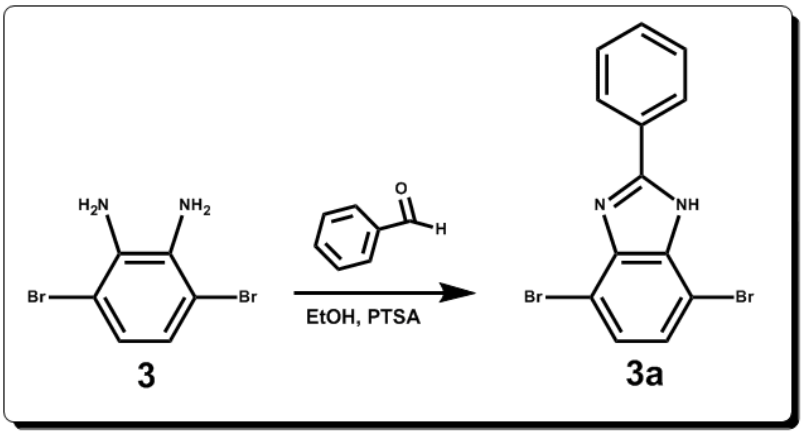

Figure 2. 3 Synthetic route for 4,7-dibromo-2-phenyl-1H-benzo[d]imidazole (**3a**).

4,7-Dibromo-2-phenyl-1H-benzo[d]imidazole was synthesized according to the literature [57]. 3,6-Dibromobenzene-1,2-diamine (500 mg, 1.88 mmol), benzaldehyde (798 mg, 7.52 mmol) and catalytic amount of PTSA were mixed in EtOH (25 ml). The mixture was left to reflux at 100 ^{o}C overnight. Solvent was removed under vacuum and the crude product was purified by column chromatography over silica gel 7:1 (chloroform:hexane) to obtain **3a** as a white solid in yield 67% (443 mg, 1.26 mmol). ^{1}H (400 MHz, $CDCl_3$, δ): 8.03 (m, 2H), 7.43 (m, 3H), 7.32 (s, 2H).

2.3.4 Synthesis of 2,3-dihydrothieno[3,4 b][1,4]dioxine-5-carbaldehyde (5)

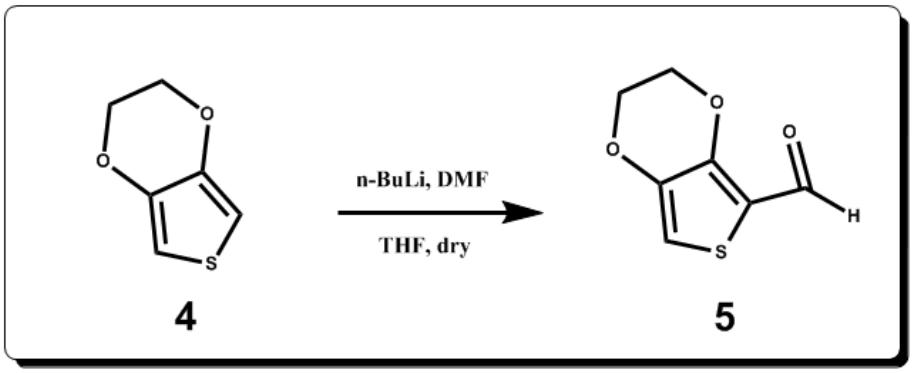

Figure 2. 4 Synthetic route for 2,3-dihydrothieno[3,4 b][1,4]dioxine-5-carbaldehyde (**5**).

EDOT (**4**) (2 g, 14.07 mmol) was dissolved in dry THF (30 ml) in a round bottom flask. n-BuLi (6.30 ml) was added drop-wise to the solution at -78^{o}C. The mixture was stirred for 30 min at 0^{o}C. Anhydrous DMF (2.04 ml) was added quickly to the solution at -78^{o}C and stirred for 5 min. After the solution was stirred an additional 1 h at room temperature, it was poured into icy water and acidified with HCl. Precipitate was filtered and washed with water. The product was re-crystallized in MeOH and filtered through a suction filter. 1.47 g, 8.64 mmol **5** was obtained as a reddish brown solid in yield 67%. ^{1}H NMR ($CDCl_3$) δ 9.91 (s, 1H), 6.80 (s, 1H), 4.37 (m, 2H), 4.28 (m, 2H). ^{13}C NMR ($CDCl_3$) δ 179.1, 147.3, 140.8, 117.5, 109.7, 64.4, 63.4.

2.3.5 Synthesis of 4,7-dibromo-2-(2,3-dihydrothieno[3,4-b][1,4]dioxin-5-yl)-1H-benzo [d]imidazole (3b)

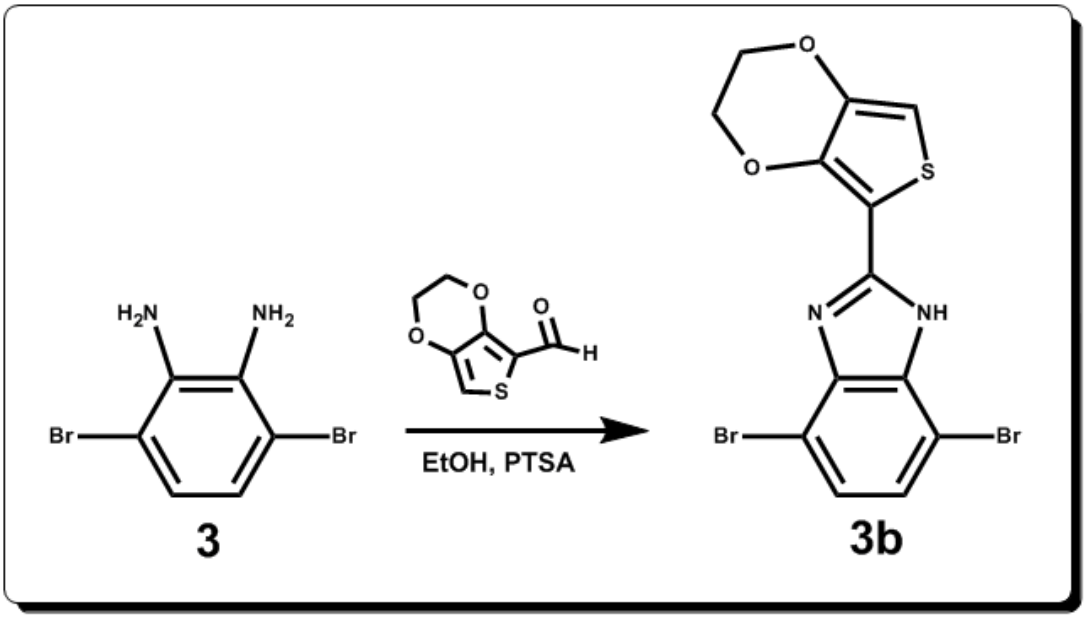

Figure 2. 5 Synthetic route for 4,7- dibromo-2-(2,3-dihydrothieno[3,4-b][1,4]dioxin-5-yl)-1H-benzo [d]imidazole (**3b**).

4,7-Dibromo-2-(2,3-dihydrothieno[3,4-b][1,4]dioxin-5-yl)-1H-benzo [d]imidazole was synthesized according to the same procedure described for **3a** [57]. 3,6-Dibromobenzene-1,2-diamine (500 mg, 1.88 mmol), 2,3-dihydrothieno[3,4 b][1,4]dioxine-5-carbaldehyde (**5**) (320 mg, 1.88 mmol) and catalytic amount of PTSA were mixed in EtOH (25 ml). The mixture was left to reflux at 100^{o}C overnight. Solvent was removed under vacuum and the crude product was purified by column chromatography over silica gel 1:1 (ethylacetate:hexane) to obtain **3b** as pale yellow solid in yield 63% (493 mg, 1.18 mmol). ^{1}H (400 MHz, $CDCl_3$, δ): 9.85 (s, 1H), 7.21 (s, 2H), 6.5 (s, 1H), 4.36 (m, 4H).

2.3.6 Synthesis of 4,7-Dibromo-2-ferrocenyl-1H-benzo[d]imidazole (3c)

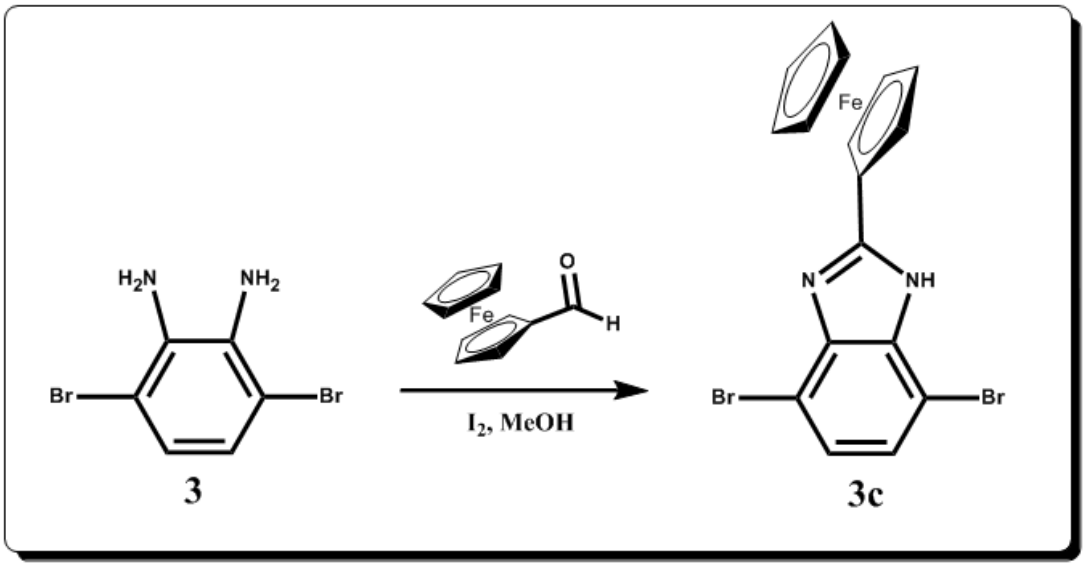

Figure 2. 6 Synthetic route for 4,7-Dibromo-2-ferrocenyl-1H-benzo[d]imidazole (**3c**).

3,6-Dibromobenzene-1,2-diamine (**3**) (500 mg, 1.88 mmol) and ferrocene carboxaldehyde (483 mg, 2.41mmol) were dissolved in 30 ml methanol (MeOH). After clear solution was obtained, 20 mg iodine were added to the mixture and stirred at room temperature overnight. Subsequent precipitate was filtered and washed with cold MeOH (3 x 50ml). The product was obtained as orange solid (530mg, yield: 77%) after re-crystallization in MeOH. 1H (400 MHz, DMSO-d6, d): 12.80 (s,1H), 7.30 (m, 2H), 5.26 (t, 2H), 4.53 (t, 2H), 4.15 (s, 5H). 13C
NMR (100 MHz, DMSO-d6, d): 155.4, 142.9, 134.8, 133.3, 132.1, 125.4, 125.3, 110.1, 105.6, 101.7, 101.6, 99.5, 79.1, 72.8, 70.3, 69.5, 68.0.

2.3.7 Synthesis of tributyl(2,3-dihydrothieno[3,4-b][1,4]dioxin-7-yl)stannane (6)

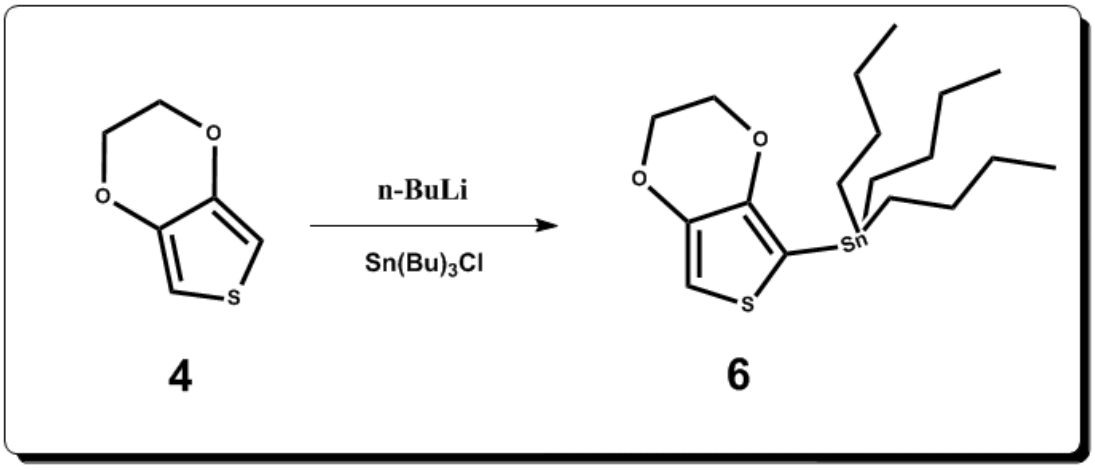

Figure 2. 7 Synthetic route for tributyl(2,3-dihydrothieno[3,4-b][1,4]dioxin-7-yl)stannane (**6**).

Tributyl(2,3-dihydrothieno[3,4-b][1,4]dioxin-7-yl)stannane was synthesized according to the literature [55]. EDOT (4.0 g, 28.1 mmol) was dissolved in dry THF (80 ml) in a round bottom flask and vacuumed for 5 min. n-BuLi (7.9 g, 122.8 mmol) was added dropwise to the solution at -78^{o}C. After addition completed, the mixture was left to stir for 1 h at room temperature. $Sn(Bu)_3Cl$ (9.2 g, 28.1 mmol) was added drop-wise at -78^{o}C and the solution was left to warm to room temperature. After stirring 24 h, 100 ml water was added to the solution. The product was extracted with DCM. Organic layer was dried over $MgSO_4$ and the solvent was removed under vacuum. The product was obtained as a viscous brown liquid. ^{1}H NMR ($CDCl_3$) δ 6.56 (s,1H), 4.16 (s, 4H), 1.61-1.49 (m, 6H), 1.39-1.22 (m, 6H), 1.09(m, 9H), 0.9 (m, 6H). ^{13}C NMR ($CDCl_3$) δ 147.88, 142.65, 109.8, 105.99, 64.86, 64.80, 29.08, 27.40, 13.76, 10.72.

2.3.8 Synthesis of 4-(2,3-Dihydrothieno[3,4-b][1,4]dioxin-5-yl)-7-(2,3 dihydrothieno[3,4b][1,4] dioxin-7-yl)-2-benzyl-1H-benzo[d]imidazole (M1)

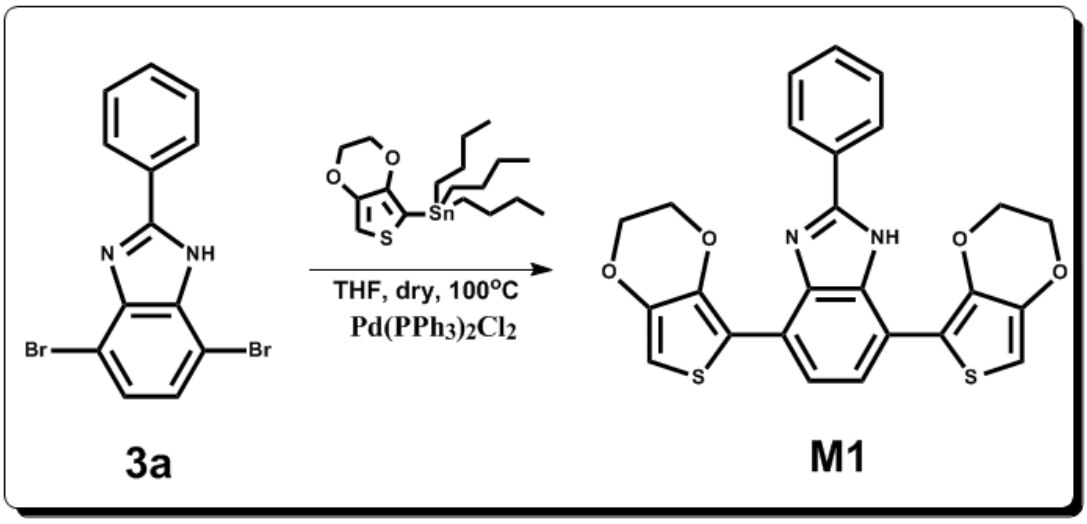

Figure 2. 8 Synthetic route for 4-(2,3-Dihydrothieno[3,4-b][1,4]dioxin-5-yl)-7-(2,3 dihydrothieno[3,4b][1,4] dioxin-7-yl)-2-benzyl-1H-benzo[d]imidazole (**M1**).

In a three necked round-bottom flask fitted with a condenser and argon inlet, 4,7-dibromo-2-phenyl-1H-benzo[d]imidazole (100 mg, 0.28 mmol) and tributyl(2,3-dihydrothieno[3,4-b][1,4]dioxin-7-yl)stannane (490 mg, 1.14 mmol) were dissolved in 25 ml of dry THF. After 30 min stirring under argon flow, dichlorobis(triphenyl phosphine) palladium(II) (30 mg, 0.027 mmol) was added at room temperature. The mixture was left to reflux for 18 h. Solvent was evaporated under vacuum and the crude product was purified by column chromatography over silica gel 1:2 (ethylacetate:hexane) to obtain M1 as yellow solid (78 mg, yield: 58.7 %). ^{1}H (400 MHz, $CDCl_3$, δ): 10.61 (s, 1H), 8.09 (d, 2H), 8.05 (d, 1H), 7.50 (m, 3H), 7.42 (d, 1H), 6.52 (s, 1H), 6.44 (s, 1H), 4.48 (d, 2H), 4.38 (d, 4H), 4.29 (d, 2H). ^{13}C NMR (100 MHz, $CDCl_3$, δ): 150.4, 142.0, 141.5, 141.1, 139.5, 135.9, 131.5, 130.2, 129.9, 129.0, 128.2, 126.4, 125.3, 123.9, 121.3, 120.7, 116.7, 114.6, 114.5, 100.9, 99.2, 65.6, 64.9, 64.5, 64.4. MS (*m*/*z*): 475 [M+].

2.3.9 Synthesis of 2,4-bis(2,3-dihydrothieno[3,4-b][1,4]dioxin-5-yl)-7-(2,3-dihydrothieno[3,4-b][1,4]dioxin-7-yl)-1H-benzo[d]imidazole (M2)

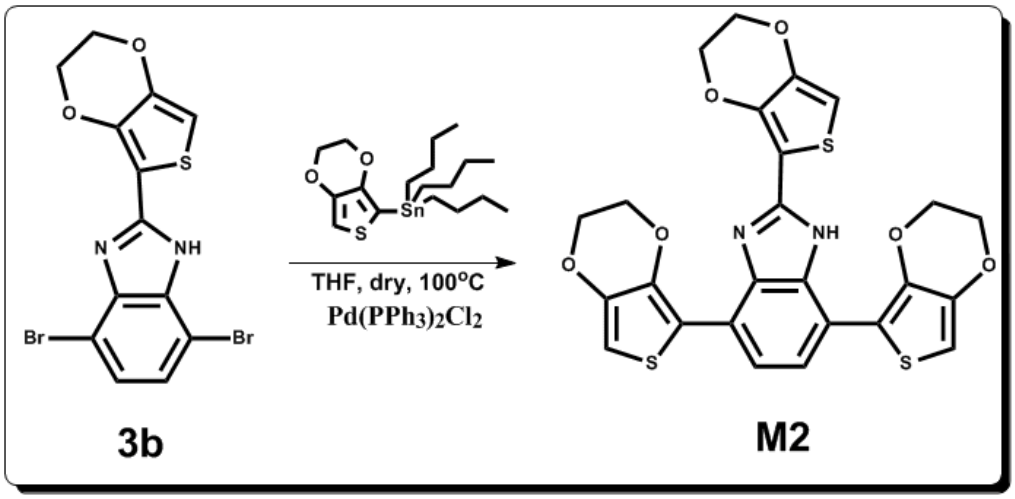

Figure 2. 9 Synthetic route for 2,4-bis(2,3-dihydrothieno[3,4-b][1,4]dioxin-5-yl)-7-(2,3-dihydrothieno[3,4-b][1,4]dioxin-7-yl)-1H-benzo[d]imidazole (**M2**).

This monomer was prepared with the same procedure described for **M1** using 4,7-dibromo-2-(2,3-dihydrothieno[3,4-b][1,4]dioxin-5-yl)-1H-benzo[d]imidazole (200 mg, 0.48 mmol), tributyl(2,3-dihydrothieno[3,4-b][1,4]dioxin-7-yl)stannane (829.1 mg, 1.92 mmol), and dichlorobis(triphenyl phosphine)palladium(II) (50 mg, 0.045 mmol) in 35 ml of dry THF. After removing the solvent on rotary evaporator, the residue was subjected to column chromatography on silica gel, eluting with 1:1 (ethyl acetate:hexane) to obtain **M2** as yellow solid (156 mg, yield: 60.3 %).^{1}H (400 MHz, $CDCl_3$, δ): 10.86 (s, 1H), 8.02 (d, 1H), 7.38 (d, 1H), 6.50 (s, 1H), 6.49 (s, 1H), 6.43 (s, 1H), 4.36 (m, 12H). ^{13}C NMR (100 MHz, $CDCl_3$, δ): 145.2, 143.9, 140.9, 140.3, 139.7, 139.2, 135.5, 129.1, 127.3, 124.6, 120.5, 119.7, 114.9, 114.1, 110.3, 107.9, 101.9, 101.3, 98.7, 64.7, 64.6, 64.3, 63.3, 63.2. MS (*m*/*z*): 539 [M+].

2.3.10 Synthesis of 4-(2,3-dihydrothieno[3,4-b][1,4]dioxin-5-yl)-7-(2,3-dihydrothieno[3,4-b][1,4]dioxin-7-yl)-2-ferrocenyl-1H-benzo[d]imidazole (M3)

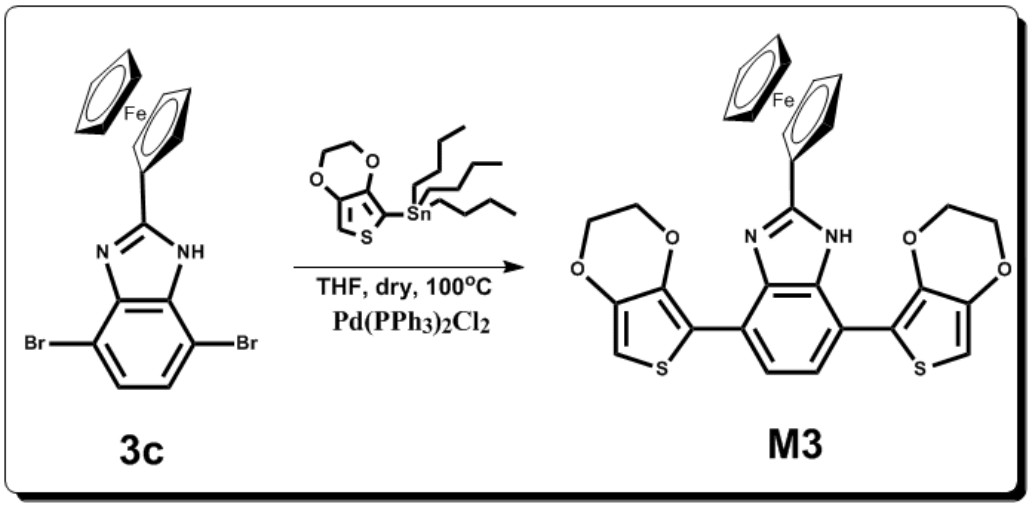

Figure 2. 10 Synthetic route for 4-(2,3-dihydrothieno[3,4-b][1,4]dioxin-5-yl)-7-(2,3-dihydrothieno[3,4-b][1,4]dioxin-7-yl)-2-ferrocenyl-1H-benzo[d]imidazole (**M3**).

This compound was also prepared with the same procedure described above, using 4,7-dibromo-2-ferrocenyl-1H-benzo[d]imidazole (500 mg, 1.08 mmol), tributyl(2,3-dihydrothieno[3,4-b][1,4]dioxin-7-yl)stannane (829.1 mg, 1.92 mmol), and dichlorobis(triphenyl phosphine)palladium(II) (70 mg, 0.064 mmol) in 50 ml of dry THF. In this case completion of the reaction was achieved by an additional 30 h of reflux as monitored by TLC. Solvent was removed under vacuum and the crude product was purified by column chromatography over silica gel 1:3 (ethylacetate:hexane) to obtain **M3** as orange solid (430 mg, yield: 68 %). ^{1}H (400 MHz, DMSO-d_6, δ): 11.69 (s, 1H), 7.92 (d, 1H), 7.09 (d, 1H), 6.75 (s, 1H), 6.69 (s, 1H), 5.22 (t, 2H), 4.48 (t, 2H), 4.39 (m, 4H), 4.28 (m, 4H), 4.14 (s, 5H). ^{13}C NMR (100 MHz, DMSO-d_6, δ): 152.7, 142.2, 141.3, 140.1, 139.1, 138.4, 132.4, 124.3, 122.0, 121.5, 119.1, 113.8, 112.6, 100.7, 98.8, 79.3, 79.1, 78.9, 78.6, 74.2, 69.8, 69.4, 67.9, 67.8, 64.8, 64.6, 64.2, 64.0, 56.0. MS (*m*/*z*): 583 [M+].

CHAPTER 3

RESULTS AND DISCUSSION

3.1 Electrochemical and Electrochromic Properties of Benzimidazole Derivative Polymers

3.1.1 Electropolymerization of Monomers (M1, M2 and M3)

All polymerizations were performed using a three electrode system by applying multiple scan voltammetry at a scan rate of 100 mV/s.

3.1.1.1 Electropolymerization of (M1)

M1 was polymerized potentiodynamically on ITO coated glass slide in a mixture of dichloromethane (DCM) and acetonitrile (ACN) (5/95, v/v) using 0.1 M tetrabutylammonium hexafluorophosphate ($TBAPF_6$) as the supporting electrolyte with repeated scan interval between -300 mV and 1200 mV (Figure 3.1).

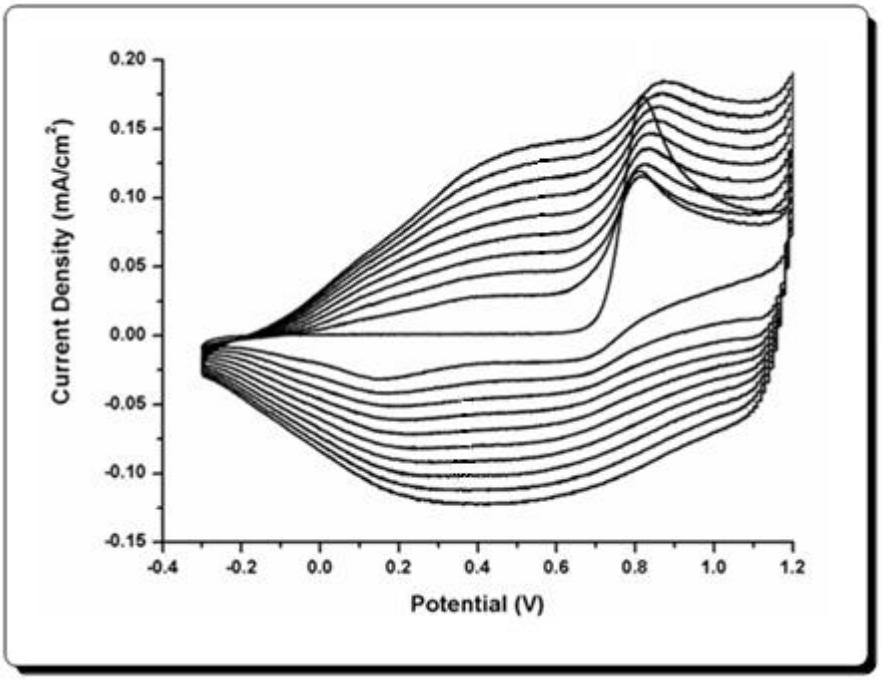

Figure 3. 1 Electropolymerization of **P1**.

In the first cycle of voltammogram, an irreversible monomer oxidation peak at 0.82 V appeared and a reversible polymer redox peak was centered at 0.56 V and 0.38 V versus Ag wire pseudo reference electrode. As seen in the Figure 3.1, current density increases with increasing number of cycle which proves the formation of the polymer on ITO surface.

3.1.1.2 Electropolymerization of (M2)

M2 was polymerized potentiodynamically in the same electrolytic medium used for **M1** on ITO coated glass slide in a mixture of dichloromethane (DCM) and acetonitrile (ACN) (5/95, v/v) using 0.1 M tetrabutylammonium hexafluorophosphate ($TBAPF_6$) as supporting electrolyte with repeated scan interval between -300 mV and 900mV (Figure 3.2).

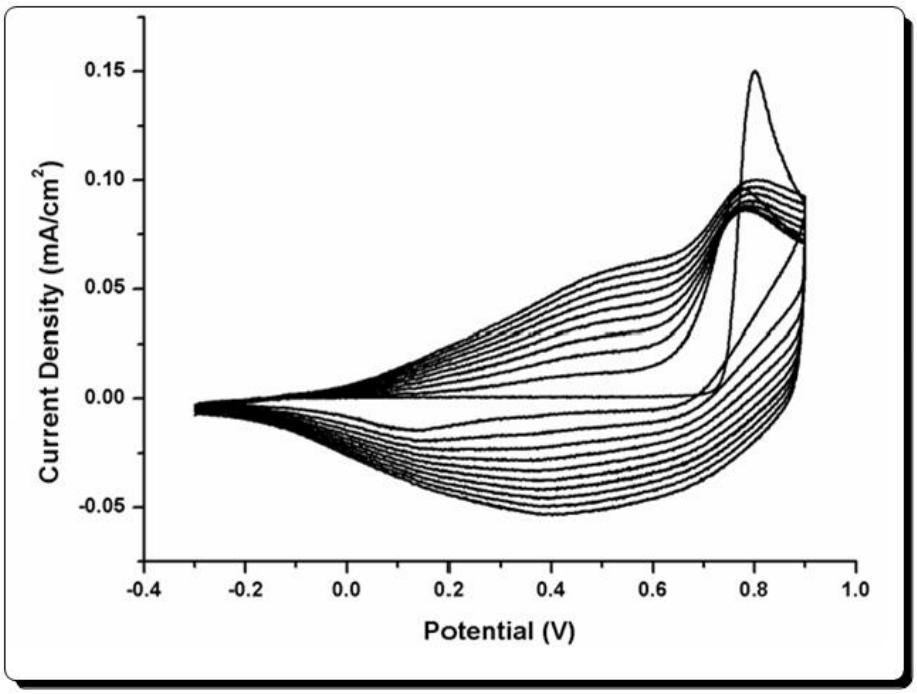

Figure 3. 2 Electropolymerization of **P2**.

An irreversible monomer oxidation peak appeared at 0.80 V in the first cycle of voltammogram. Polymer p-doping/dedoping potentials were lower (0.51 and 0.33 V) as benzene was replaced by electron rich 3,4-ethylenedioxy thiophene (EDOT) unit.

3.1.1.3 Electropolymerization of (M3)

M3 was also polymerized using same conditions described for **M1** and **M2**, with repeated scan interval between -500 mV and 1250 mV (Figure 3.3).

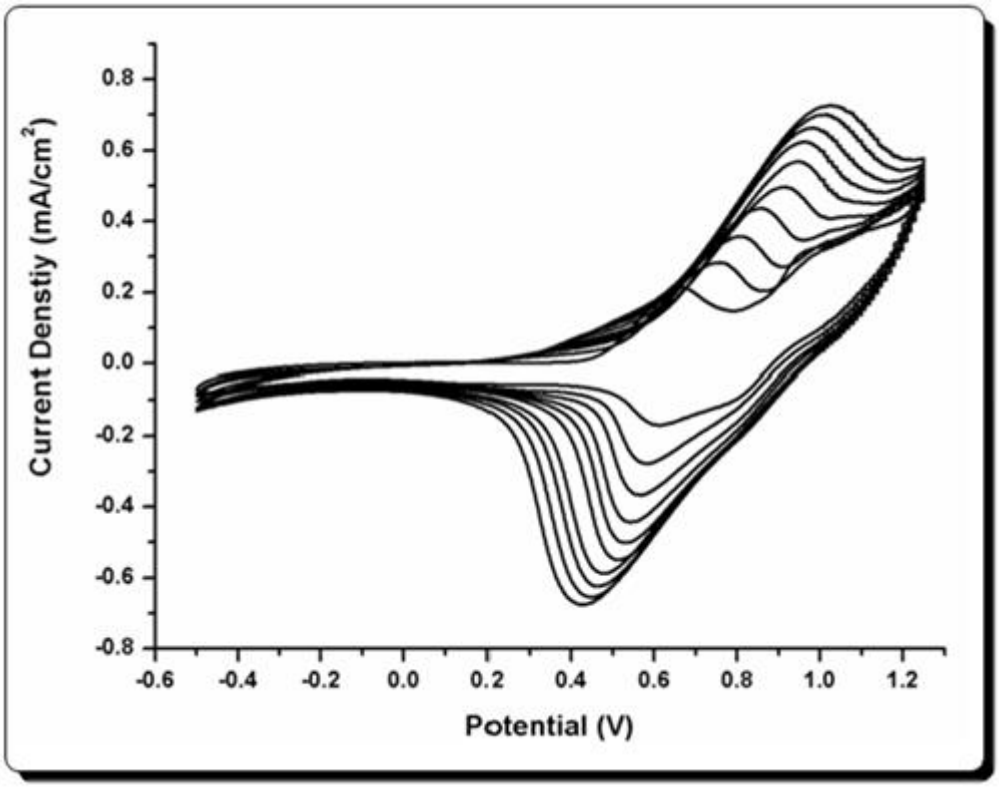

Figure 3. 3 Electropolymerization of **P3**.

During stepwise oxidation of **M3**, first peak for the ferrocenyl unit oxidation was seen at 0.65 V and the monomer oxidation peak was appeared at 0.96 V. After monomer oxidation, a reduction appeared at 0.6 V. This reduction leads to electrode surface passivation hampering to observe the ferrocene reduction peak. Nonetheless, after repetitive cycles of electropolymerization this reduction peak became visible since polymer reduction peak shifted to less positive potentials. The big difference between doping/dedoping (1.06/0.40 V) potentials for **P3** confirms a multi-electron redox process due to electroactive and bulky ferrocenyl substituents on BIm units. These bulky groups also affect the insertion of the electrolyte anion to the polymer film and the rate of quinoid to benzenoid transformation.

The difference between the oxidation potentials of **M1**, **M2** and **M3** can not be simply explained by the electron density and the electron donating capacity of the

substituents, since all the three substituents are expected to affect the planarity of the imidazole ring differently.

Corresponding polymers, **P1**, **P2** and **P3** were subjected to scan rate alternation experiments in order to determine diffusion dependencies of thin films on the working electrodes (ITO) (Figure 3.4). Linear relationships between scan rates and current intensities showed that all polymers were well adhered on ITO surface and the electrochemical processes were not limited by diffusion control [58].

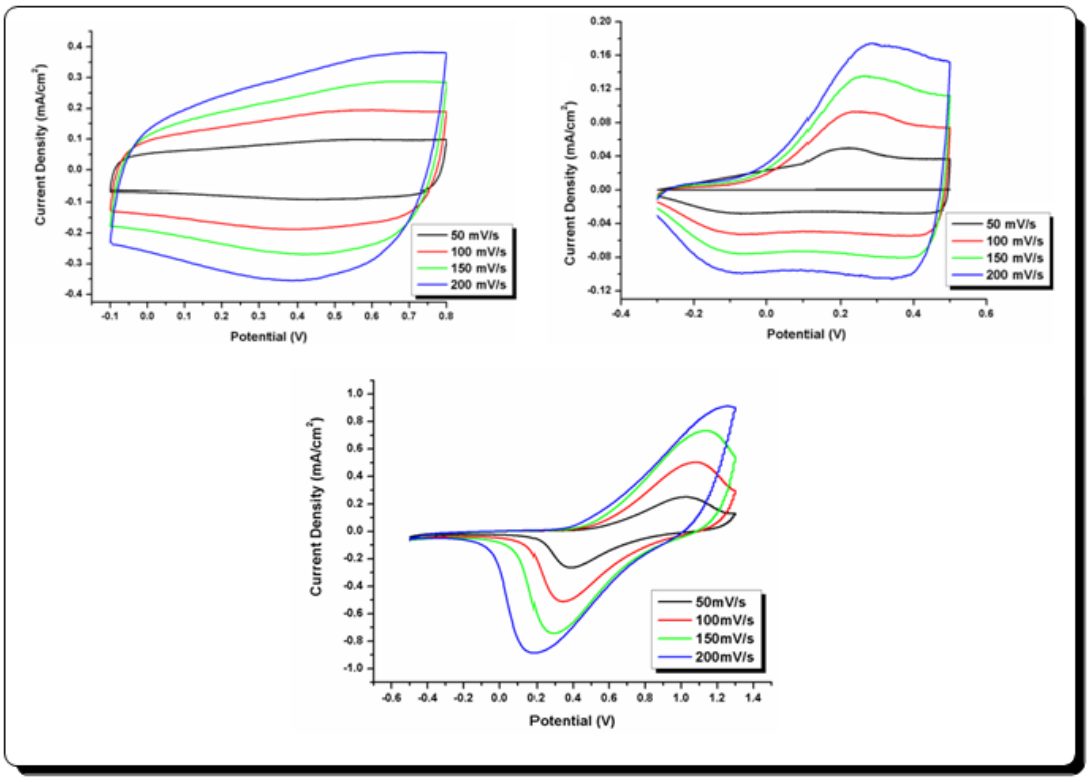

Figure 3. 4 Scan rate dependencies of corresponding polymers **P1**, **P2** and **P3**.

3.1.2 Spectroelectrochemistry of Polymers (P1, P2 and P3)

Spectroelectrochemical studies of the polymers were performed in order to examine their optical and structural responses upon doping process which proves the evolution of the charge carries in the structure. UV-vis-NIR spectra for electrochemically coated polymer films acquired during stepwise oxidation in a monomer free, 0.1 M $TBAPF_6$ / ACN solution.

3.1.2.1 Spectroelectrochemistry of P1

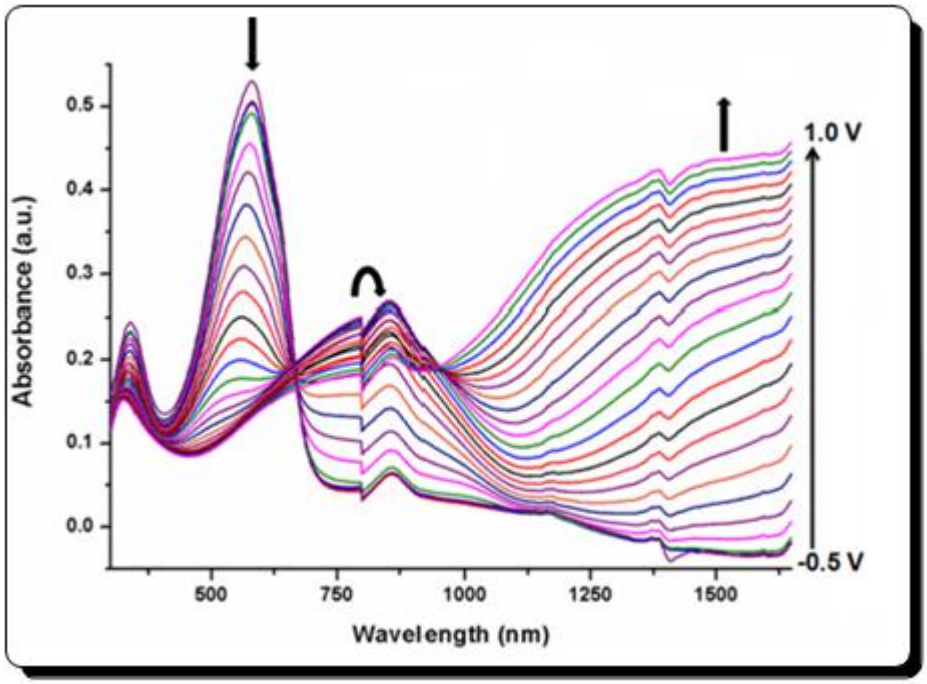

Figure 3. 5 Electronic absorption spectra of P1 film in 0.1 M $TABPF_6$/ACN solution between -0.5 V and 1.0 V with 0.05 V potential intervals.

A neutral state absorption maximum for **P1** was recorded as 580 nm. Upon oxidation of **P1** formation of charge carriers such as polarons and bipolarons [59] led to new absorption bands in NIR while absorption for the neutral state was decreasing

(Figure 3.5). In-situ spectroelectrochemical study for the polymer film showed that the color of the film changed from saturated blue to highly transmissive sky-blue (Figure 3.6).

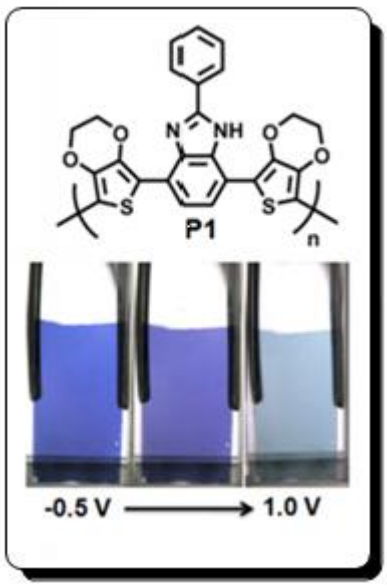

Figure 3. 6 Colors of P1 at neutral and different oxidized states.

3.1.2.2 Spectroelectrochemistry of P2

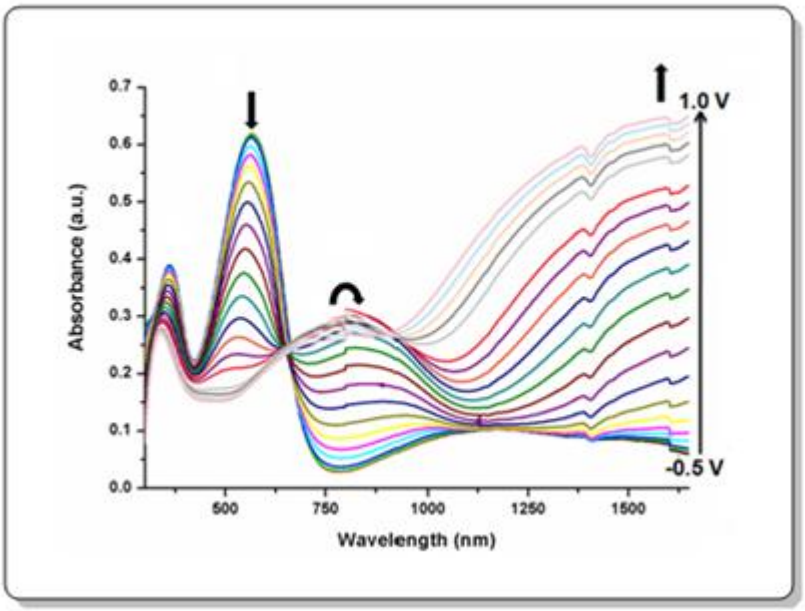

Figure 3. 7 Electronic absorption spectra of P2 film in 0.1 M $TABPF_6$/ACN solution between -0.5 V and 1.0 V with 0.05 V potential intervals.

A neutral state absorption maximum for **P2** was recorded as 560 nm. Upon step-wise oxidation a highly transmissive sky-blue oxidized state was observed. **P2** revealed different shades and tones as the transition colors since polaronic absorption bands tailed more into the visible region (Figure 3.7). Although both **P1** and **P2** showed identical polaronic absorptions, these bands decreased less with increasing potential for **P2** than those of **P1** due to simultaneous formation of polaronic and bipolaronic charge carriers. Additionally, isosbestic point at around 650 nm for **P2** confirmed the coexistence of more than one charged species absorbing in the visible region on the polymer chain. These different species contribute differently to the resulting color of the film in the sense that as if one mixes two different colored polymers [60]. As their absorption bands respond differently upon stepwise oxidation, multicolored states are achieved. It can also be generalized that polymers having isosbestic points usually result in multicolored achievable states [61].

Figure 3. 8 Colors of **P2** at neutral and different oxidized states.

3.1.2.3 Spectroelectrochemistry of P3

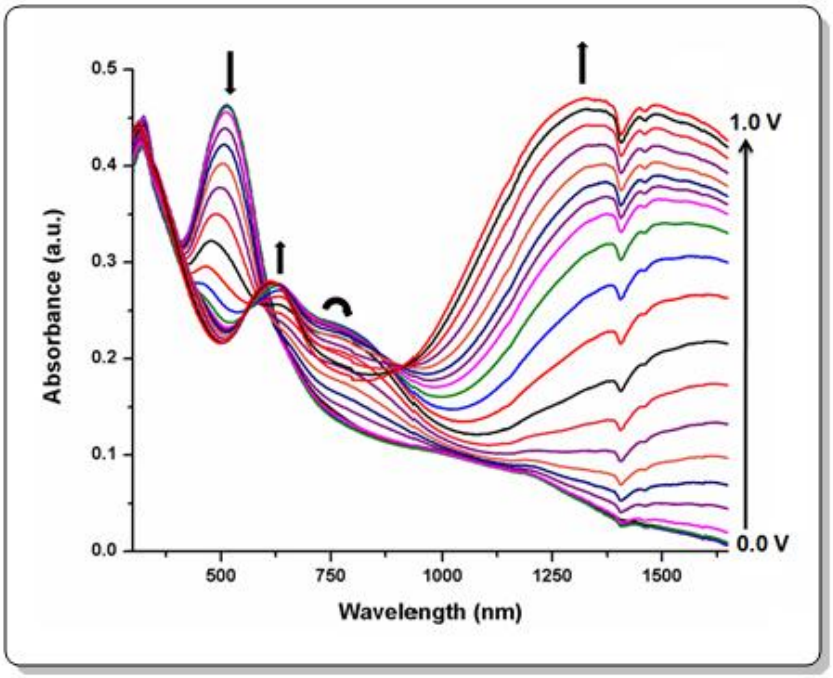

Figure 3. 9 Electronic absorption spectra of P3 film in 0.1 M $TABPF_6$/ACN solution between 0.0 V and 1.0 V with 0.05 V potential intervals.

A neutral state absorption maximum for **P3** was recorded as 513 nm. Color of **P3** in its different redox states were affected by the bulky and visible absorber Fc pendant group. Oxidation of **P3** film resulted in a similar behavior to **P1** and **P2** at its early doping stages, but later a new absorption band was emerged at 625 nm which stands for polaronic absorption bands (770 nm) with increasing bias due to characteristic blue color of Fc^+ ions. This visible absorption of Fc^+ groups conduced with a blue colored oxidized state for **P3** film. Moreover, partial oxidation of **P3** allowed detection of a gray colored transition state as a consequence of mixing different colored states of main chain and Fc groups (Figure 3.9 and 3.10).

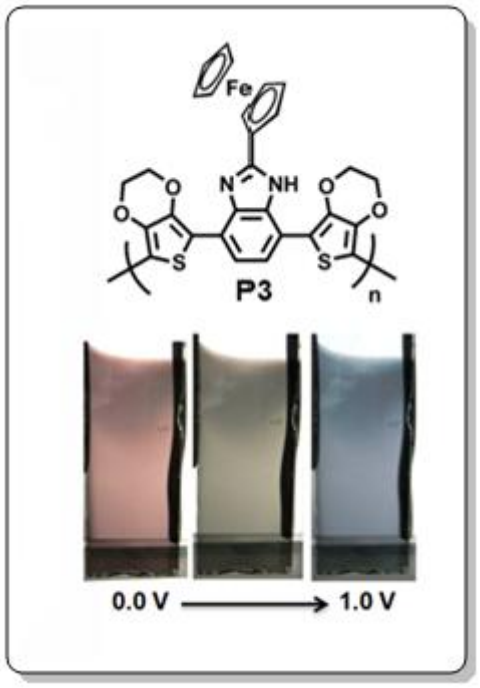

Figure 3. 10 Colors of **P3** at neutral and different oxidized states.

Optical band gaps of the polymers were calculated as 1.75, 1.69 and 1.77 eV for **P1**, **P2** and **P3** respectively from the onset of π-π* transitions in the visible region.

Although BIm based polymers exhibited two transitions due to their donor-acceptor nature, the lowest energy transitions affected the colors of neutral films dominantly

since other transitions were not in the visible region. The two transitions for DAD type polymers are attributed to the transitions from the thiophene-based valence band to its antibonding counterpart (high-energy transition) and to the substituent-localized conduction band (low-energy transition) hence, interactions between donor and acceptor units (their match) determine the energy and intensity of these transitions. This phenomenon is in agreement with the blue shifts and decreasing intensity for series of polymers with decreasing acceptor strengths.

3.1.3 Kinetic Studies of Polymers (P1, P2 and P3)

Optical contrasts were monitored as the function of time at the maximum absorption of **P1**, **P2** and **P3** in order to characterize their response times and switching abilities. Electrochemically polymerized films were subjected to chronoabsorptometry studies in a monomer free solution containing 0.1 M $TBAPF_6$/ACN.

3.1.3.1 Kinetic Study of Polymer P1

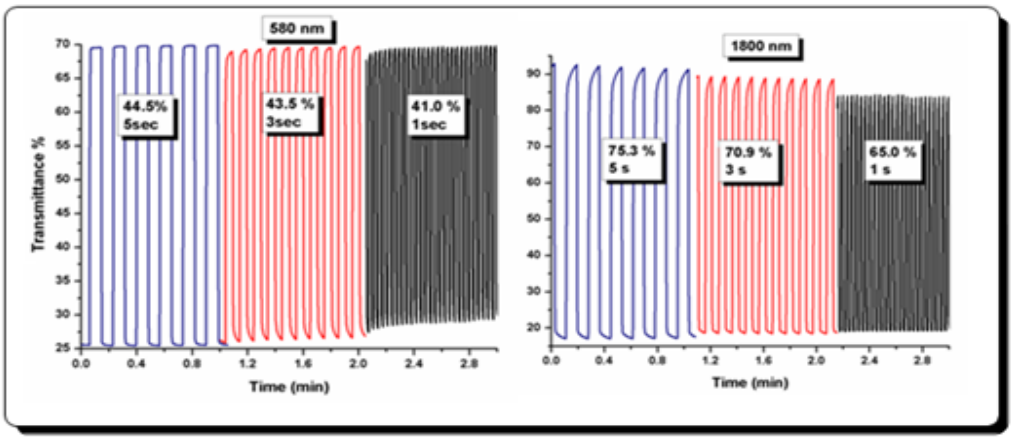

Figure 3. 11 Square wave potential step chronoabsorptometry study of P1 monitored at 580 nm and 1800 nm between -0.5 V and 1.0 V (vs. Ag wire). Switching time intervals: 5 s, 3 s and 1 s.

Switching abilities of **P1** were measured at its highest absorption values in visible and NIR regions. As depicted in (Figure 3.11), **P1** revealed optical contrast value of 45 % at its short wavelength maximum absorption at 580 nm and 75 % at 1800 nm. It is quite impressive and eminent to use this material in NIR applications [62].

3.1.3.2 Kinetic Study of Polymer P2

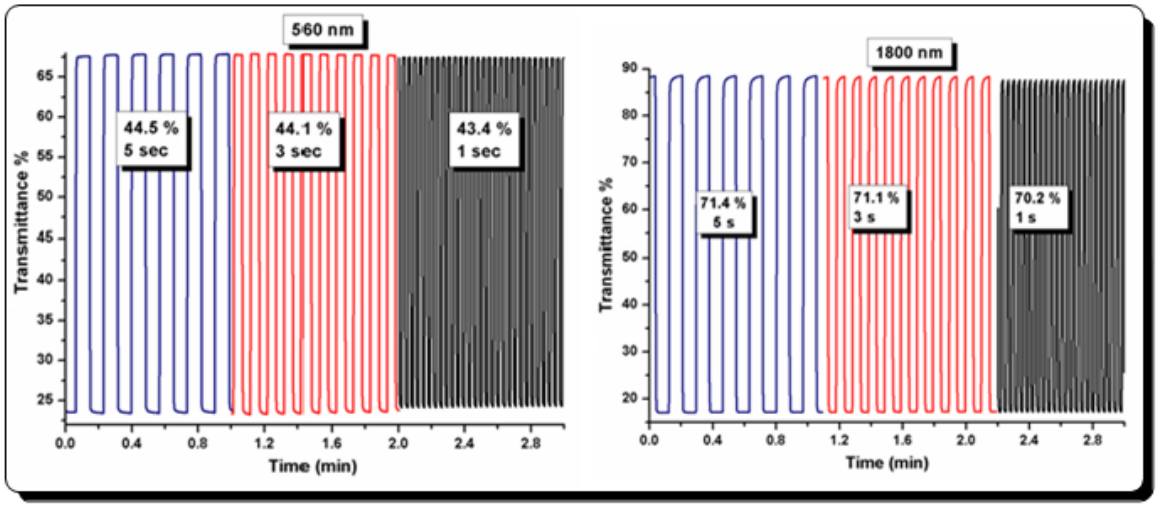

Figure 3. 12 Square wave potential step chronoabsorptometry study of P2 monitored at 560 nm and 1800 nm between -0.5 V and 1.0 V (vs. Ag wire). Switching time intervals: 5 s, 3 s and 1 s.

44.5 % and 71.4 % optical contrast values were determined for **P2** at 560 nm and 1800 nm. **P2** did not exhibit a difference in its optical contrast values (44.5 % => 43.6 %) even though the switching time was changed to 1 second. Although for **P1** a variation in electrochromic contrast of 4 % was observed as the stepping interval was changed from 5 to 1 second, **P2** revealed the robustness and the stability of the material applications like electrochromic devices and optical displays.

3.1.3.3 Kinetic Study of Polymer P3

Among others, **P3** showed lower optical contrast values; 10 % at 513 nm and 36 % at 1370 nm, when switched between its neutral and oxidized states. **P3** showed trapezoidal pulses which resulted in longer switching times (2.5 s) (Figure 3.13).

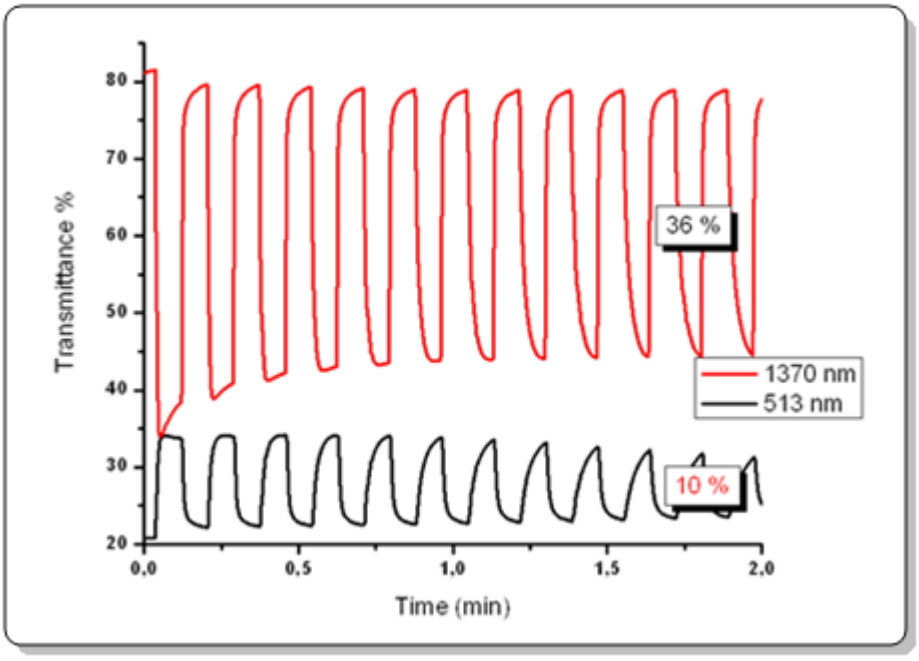

Figure 3. 13 Square wave potential step chronoabsorptometry studies of P3 monitored at 1800 nm between 0.0 V and 1.0 V (vs. Ag wire reference electrode). Switch interval: 5 s.

Table 1 summarizes the switching abilities for **P1**, **P2** and **P3** at their dominant wavelengths in visible and NIR regions. As seen, for **P1** and **P2**, it does not matter how fast the polymer films were switched, the time required to switch between their neutral and oxidized states did not change significantly which also can be an evidence for the durability of the polymer films.

Table 1 Optical contrasts and switching abilities of polymers **P1**, **P2** and **P3**.

	Switching Intervals	T_{red} %	T_{ox} %	ΔT %	t_{ox} (s)
P1 λ_{max}: 580 nm	5 s	25.2	69.7	44.5	0.42
	3 s	26.0	69.5	43.5	0.60
	1 s	27.9	68.9	41.0	0.40
P1 λ_{max}: 1800 nm	5 s	17.2	92.5	75.3	0.62
	3 s	18.5	89.4	70.9	0.60
	1 s	18.8	83.8	65.0	0.52
P2 λ_{max}: 560 nm	5 s	23.2	67.9	44.5	0.48
	3 s	23.6	67.7	44.1	0.40
	1 s	24.0	67.4	43.4	0.42
P2 λ_{max}: 1800 nm	5 s	17.1	88.5	71.4	0.54
	3 s	17.3	88.4	71.1	0.36
	1 s	17.4	87.6	70.2	0.30
P3 λ_{max}: 513 nm	5 s	22.3	32.5	10.2	2.5
P3 λ_{max}: 1800 nm	5 s	41.2	79.4	38.2	2.0

CHAPTER 4

CONCLUSION

Three DAD type monomers bearing electron deficient BIm units as the acceptor and electron rich EDOT units as the donor groups were synthesized. Their electrochemically synthesized polymers on ITO coated glass slides were characterized in terms of their electrochemical and optical properties. Electrochemical studies showed that donor acceptor match between BIm and EDOT units is not strong as was the case in the other benzazole bearing DAD type polymers. However, spectroelectrochemical results proved their great candidacy for electrochromic display device applications. Altering the pendant group affected the electrochromic behavior of the resulting polymers dramatically. EDOT substitution on 2-C position of the BIm unit revealed a polymer with multicolored oxidation states within a low potential range whereas phenyl substituted polymer switched between the different shades of the same color. Ferrocene group was also incorporated into polymer chain as a pendant group and it also contributed to the color of the polymer. Reported results for all polymers prove the potential use of BIm as an acceptor unit in DAD type polymers.

This study was published in the journal Polymer in October, 2010 [63].

REFERENCES

[1] H. Letheby, *J. Chem. Soc.*, **1862**, 15, 161.

[2] H. Shirakawa, E. J. Louis, A. G. MacDiarmid, C. K. Chiang, A. J. Heeger,; *J. Chem. Soc. Chem. Commun*., **1977**, 578.

[3] C. K. Chiang, C. R. Fincher, Jr., Y. W. Park, A. J. Heeger, H. Shirakawa, E. J Louis, S. C. Gau, A. G. Macdiarmid,; *Phys. Rev. Letters*, **1977**, *39*1098.

[4] A. F. Diaz, K. K. Kanazawa, G. P. Gardini, *J. Chem. Soc., Chem. Commun,*. **1979**, 635.

[5] K. K. Kanazawa, A. F. Diaz, R. H. Geiss, W. D. Gill, J. F. Kwak, J. A. Logan, J. F. Rabolt, G. B. Street, *J. Chem. Soc., Chem. Commun.*, **1979**, 854.

[6] M. Sato, S. Tanaka, K. Kaeriyama, *J. Chem. Soc., Chem. Commun.*, **1986**, 873.

[7] K. Y. Jen, G. G. Miller, R. L. Elsenbaumer, *J. Chem. Soc., Chem. Commun*., **1986**, 1346.

[8] a) J. H. Burroughes. D. D. C. Bradley, A. R. Brown, R. N. Marks, K. Mackay, R.H. Friend, P. L. Burns, A. B. Holmes, *Nature*, **1990**, 347, 539. b) A.C. Grimsdale, K.L. Chan, R.E. Martin, P.G. Jokisz, A.B. Holmes., *Chem Rev*, **2009**, 109, 3, 897.

[9] a) A. J. Mozer, N. S. Sariciftci; *C. R. Chimie*, **2006**, 9, 568. b) S. Gunes, H. Neugebauer, N. S. Sariciftci, *Chem Rev*, **2007,** 107, 4, 1324.

[10] a) A. L. Dyer, J. R. Reynolds, Electrochromism of Conjugated Conducting Polymers. In *Handbook of Conducting Polymers*, ed.; T. A. Skotheim, J. R. Reynolds, **2006**, Ed. CRC Press: Boca Raton, FL,; Chapter 20. b) M. A. Invernale, Y. Ding, D. M. D. Mamangun, M. S. Yavuz, G. A. Sotzing., *Adv Mater*, **2010**, 22, 12, 1379.

[11] a) M. Urien, G. Wantz, E. Cloutet, L. Hirsch, P. Tardy, L. Vignau, H. Cramail, J. P. Parneix, *Organic Electronics*, **2007,** 8, 727. b) S. Allard, M. Forster, B. Souharce, H. Thiem, U Scherf., *Angew Chem Int Ed*, **2008**, 47,22, 4070.

[12] D. M. de Leeuw, M. M. J. Simenon, A. R. Brown, R. E. F. Einerhand,; *Synth. Met.* **1997,** 87, 1, 53.

[13] J. Roncali, *Chem. Rev*. **1997**, 97, 173.

[14] a) A. Berlin, A. Canavesia, G. Pagan, G. Schiavonb, S. Zecchinb, G. Zottib, *Synth. Met.*,**1997**, 84, 451. b) A. O. Patil, A. J. Heeger, F. Wudl, *Chem. Rev.*, **1988**, 88, 183.

[15] J. L. Brédas, A. J. Heeger, F. Wudl, *J. Chem. Phys.* **1986**, 85, 4673.

[16] H.A.M. Mullekom, J.A.J.M. Vekemans, E.E. Havinga and E.W. Meijer, *Mater Sci Eng*, **2001**, R32, 1.

[17] a) C.A. Thomas, K. Zong, K.A. Abboud, P.J. Steel and J.R. Reynolds, *J Am Chem Soc*., **2004**, 126, 50, 16440. b) U. Salzner and M.E. Köse, *J Phys Chem B*, **2002**, 106, 10, 9221.

[18] a) P. M. S. Monk, R. J. Mortimer, D. R. Rosseinsky, Electrochromism: Fundamentals and Applications, **1995,** Wiley-VCH. b) R. J. Mortimer, *Electrochim. Acta*, **1999,** 44.

[19] A. A. Argun, P. H. Aubert, B. C. Thompson, I. Schwendeman, C. L. Gaupp, J. Hwang, N. J. Pinto, D. B. Tanner, A. G. MacDiarmid, J. R. Reynolds; *Chem. Mater*. **2004**, 16, 4401.

[20] A. Cirpan, A.A. Argun, C.R.G. Grenier, B.D. Reeves, J.R. Reynolds, *J. Mater. Chem*., **2003,** 13, 2422.

[21] J.L. Boehme, D.S.K. Mudigonda and J.P. Ferraris, *Chem. Mater*., **2001,** 13, 4469.

[22] I. Schwendeman, J. Hwang, D.M. Welsh, D.B. Tanner, J.R.Reynolds, *Adv. Mater*. **2001,** 13, 634.

[23] I. Schwendeman, R. Hickman, G. Sonmez, P. Schottland, K. Zong, D.M. Welsh, J.R. Reynolds, *Chem. Mater*., **2002,** 14, 3118.

[24] W.A. Gazotti, G. Casalbore-Miceli, A. Geri, A. Berlin, M.A. DePaoli, *Adv. Mater.*, **1998**, 10, 1523.

[25] H. Pages, P. Topart, D. Lemordant, *Electrochim. Acta*., **2001,** 46, 2137.

[26] P. Chandrasekhar, B.J. Zay, G.C. Birur, S. Rawal, E.A. Pierson, L. Kauder, T. Swanson, *Adv. Funct. Mater*., **2002**, 12, 2137.

[27] M.A. DePaoli, W.A. Gazotti, J. Braz. *Chem. Soc*., **2002,** 13, 410.

[28] J. Roncali, *Chemical Reviews*, **1992**, 92, 4.

[29] W. J. Albery, F. Li, A. R. Mount, *Journal of Electroanalytical Chemistry and Interfacial Electrochemistry*, **1991**, 310, 1-2, 239.

[30] R. J. Waltman, J. B Argon, *Can. J. Chem.*, **1986**, 64.

[31] M. Li, Y. Sheynin, A. Patra, M. Bendikov, *Chem. Mater.* **2009,** 21, 2482.

[32] S. Ozdemir, A. Balan, D. Baran, O. Dogan, L. Toppare, *Reactive & Functional Polymers*, **2011**, 71, 168.

[33] R. D. A. Hudson, *Journal of Organometallic Chemistry*, **2001**, 47, 637.

[34] M. O. Wolf, *Adv. Mater.*, **2001**, 13, 545.

[35] C. Padeste, A. Grubelnik, L. Tiefenauer, *Biosensors & Bioelectronics*, **2000**, 15, 431.

[36] G. Zotti, S. Zecchin, G. Schiavon, *Chem. Mater.* **1995, 7,** 2309.

[37] a) S. J. Higgins, C. L. Jones, S. M. Francis, *Synthetic Metals*, **1999,** 98, 211. b) Y. Zhu, M. O. Wolf, *Chem. Mater.* **1999,** 11, 2995.

[38] G. Heywang, F. Jonas, *Adv. Mater*., **1992**, 4, 116.

[39] L. Groenendaal, F. Jonas, D. Freitag, H. Pielartzik, R. Reynolds, *Adv. Mater*., **2000,** 12, 481.

[40] C. A. Thomas, K. Zong, K. A. Abboud, P. J. Steel, J. R. Reynolds,, *J. Am. Chem. Soc.* **2004**, 126, 16440.

[41] H. A. Barker, R. D. Smyth, H. Weissbach, J. I. Toohey, J. N. Ladd, B. E. J. Volcanic, *Biol Chem*, **1960**, 235, 2, 480.

[42] S. S. Kukalenko, B. A. Bovykin, S. I. Shestakova, A. M. Omel'chenko, *Russ Chem Rev*, **1985**, 54, 7, 676.

[43] G. Ragno, A. Risoli, G. Ioele, M. de Luca, *Chem Pharm Bull*, **2006**, 54, 6, 802.

[44] S. J. Kim, E. T. Kool, *J. Am. Chem. Soc*.**, 2006**, 128, 6164.

[45] K. D. Goodwin, M. A. Lewis, F. A. Tanious, R. R. Tidwell, W. D. Wilson, M. M. Georgiadis, E. C. Long; *J. Am. Chem. Soc.* **2006**, 128, 7846.

[46] C. Rodrı´guez-Rodrı´guez, N. Sa´nchez de Groot, A. Rimola, A. Alvarez-Larena, V. Lloveras, J. Vidal-Gancedo, S. Ventura, J. Vendrell, M. Sodupe, P. Gonza´lez-Duarte; *J. Am. Chem. Soc.* **2009**, 131, 1436.

[47] M. Kawahara, M. Rikukawa, K. Sanui, *Polym. Adv. Technol.*, **2000**, 11, 544.

[48] S. Taj, S. Sankarapapavinasam, M. F. Ahmed, *Journal of Applied Polymer Science,* **2000**, 77, 112.

[49] P. Blanchard, J. M. Raimundo, J. Roncali, *Synth Met,* **2001**, 119, 527.

[50] A. Durmus, G. E. Gunbas, P. Camurlu, L. Toppare., *Chem Commun;* **2007**, 3246.

[51] A. Cihaner, F. Algı, *Adv Funct Mater,* **2008**, 18, 22, 3583.

[52] A. Balan, G. Gunbas, A. Durmus, L. Toppare, *Chem Mater,* **2008,** 20, 24, 7510.

[53] A. B. Da Silveria Neto, A. L. Santana, G. Ebeling, S. R. Goncalves, E. V. U. Costa, H. F. Quina., Dupont J, *Tetrahedron* **2005**, 61, 46, 10975.

[54] Y. Tsubata, T. Suzuki, T. Miyashi, Y. Yamashita., *J. Org. Chem* **1992**, 57, 25, 6749.

[55] S. S. Zhu, T. M. Swager., *J Am Chem Soc,* **1997**, 119, 51, 12568.

[56] B. C. Thompson, Y. G. Kim, T. D. McCarley, J. R. Reynolds, *J. Am. Chem. Soc.,* **2006**, 128, 39, 12714.

[57] T. Yamamoto, K. Sugiyama, T. Kanbara, H. Hayashi, H. Etori. *Macromol Chem Phys,* **1998**, 199, 9, 1807.

[58] G. Sonmez, I. Schwendeman, P. Schottland, K. Zong, J. R. Reynolds, *Macromolecules*, **2003**, 36, 3, 639.

[59] J. L. Bredas, R. R. Chance, R. Silbey. *Phys Rev B,* **1982,** 26, 10, 843.

[60] G. Sönmez, *Chem Commun*, **2005**, 5251.

[61] A. Balan, D. Baran, G. Gunbas, A. Durmus, F. Ozyurt, L. Toppare, *Chem Commun*, **2009**, 6768.

[62] A. M. McDonagh, S. R. Bayly, D. J. Riley, M. D. Ward, J. A. McCleverty, M. A. Cowin, C. N. Morgan, R. Varrazza, R. V. Penty, I. H. White, *Chem Mater,* **2000**, 12, 9, 2523.

[63] H. Akpinar, A. Balan, D. Baran, E. Kose Unver, L. Toppare, *Polymer*, **2010**, 51, 6123.

APPENDIX A

NMR DATA

NMR spectra were recorded on a Bruker DPX 400.

Chemical shifts δ are reported in ppm relative to $CHCl_3$ (^1H: δ=7.27), $CDCl_3$ (^{13}C: δ=77.0) and CCl_4 (^{13}C: δ=96.4) as internal standards.
^1H and ^{13}C NMR spectra of products are given below.

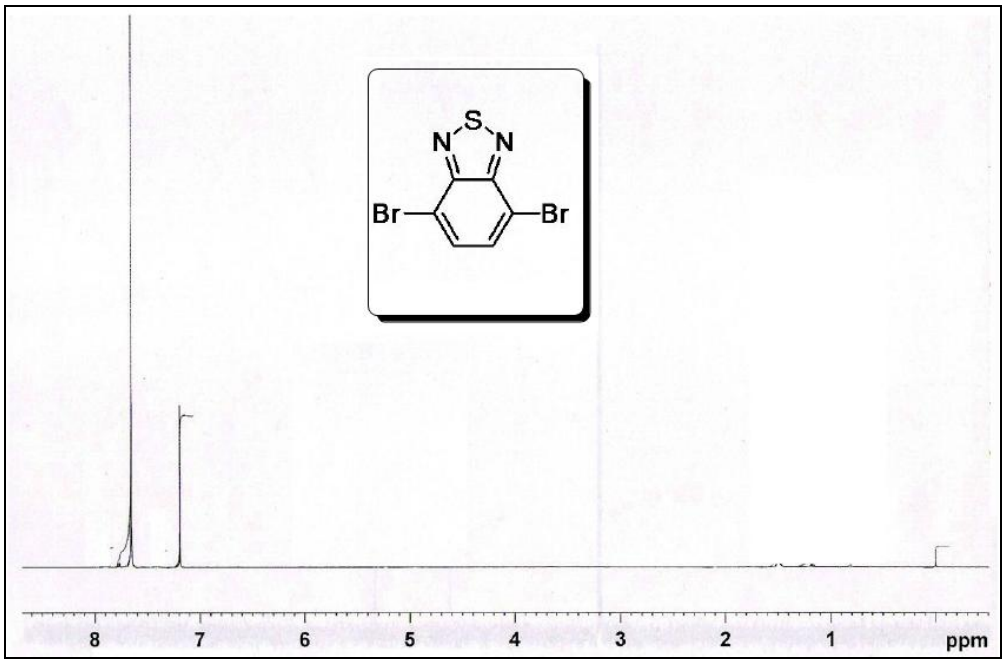

Figure A. 1 ^1H-NMR spectrum of 4,7-dibromobenzothiadiazole (**2**)

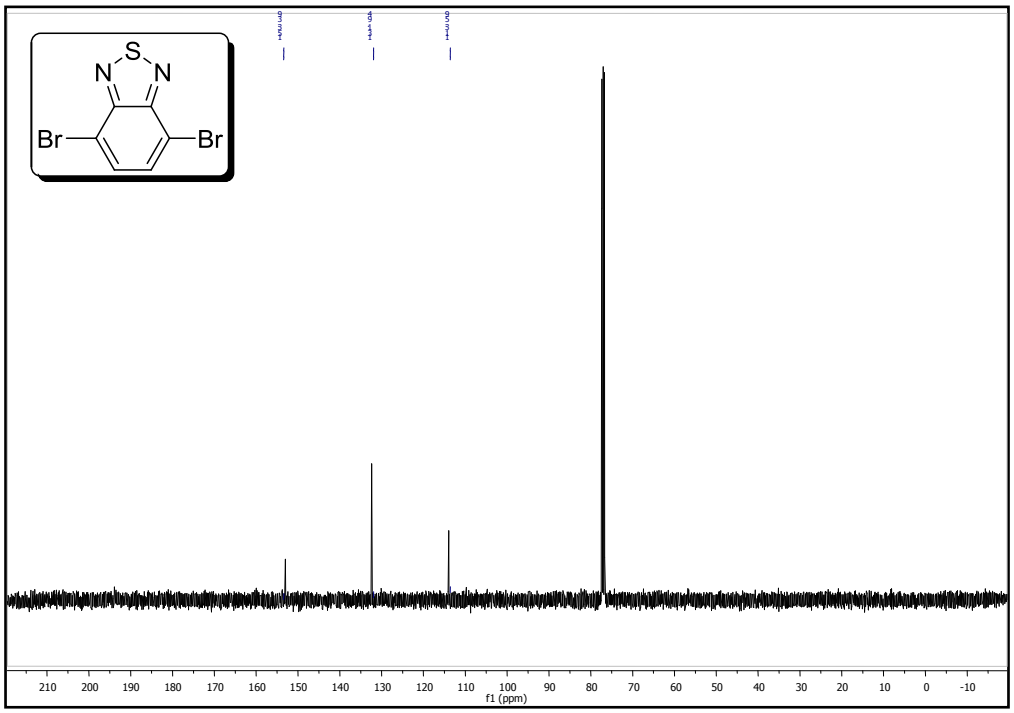

Figure A. 2 ^{13}C-NMR spectrum of 4,7-dibromobenzothiadiazole (**2**)

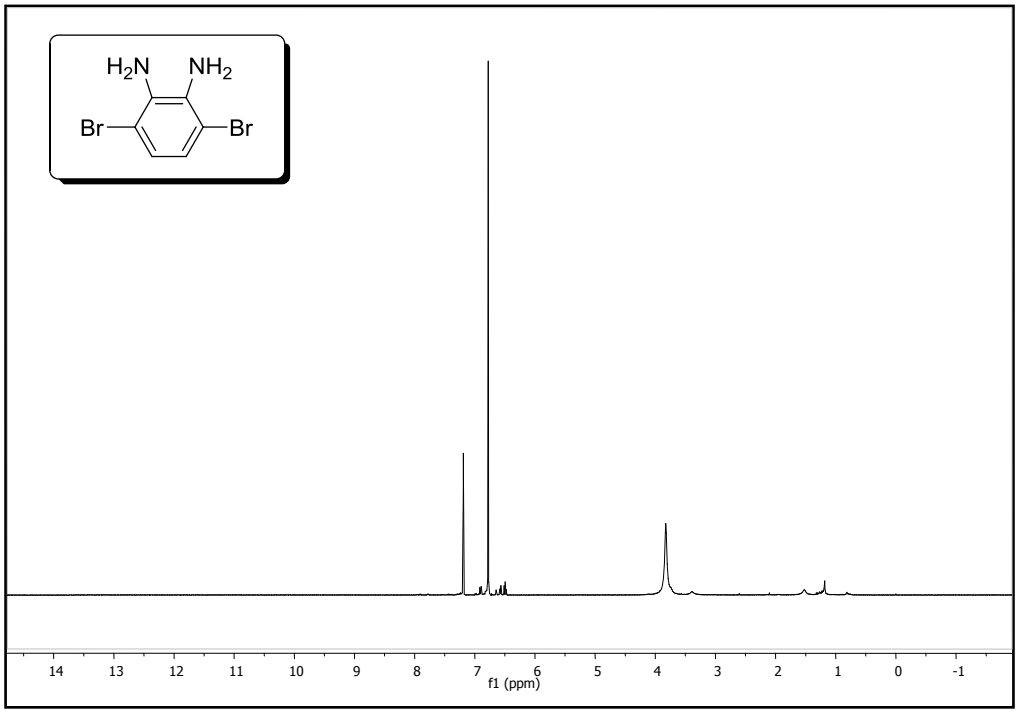

Figure A. 3 ^{1}H-NMR spectrum of 3,6-dibromobenzene-1,2-diamine (**3**)

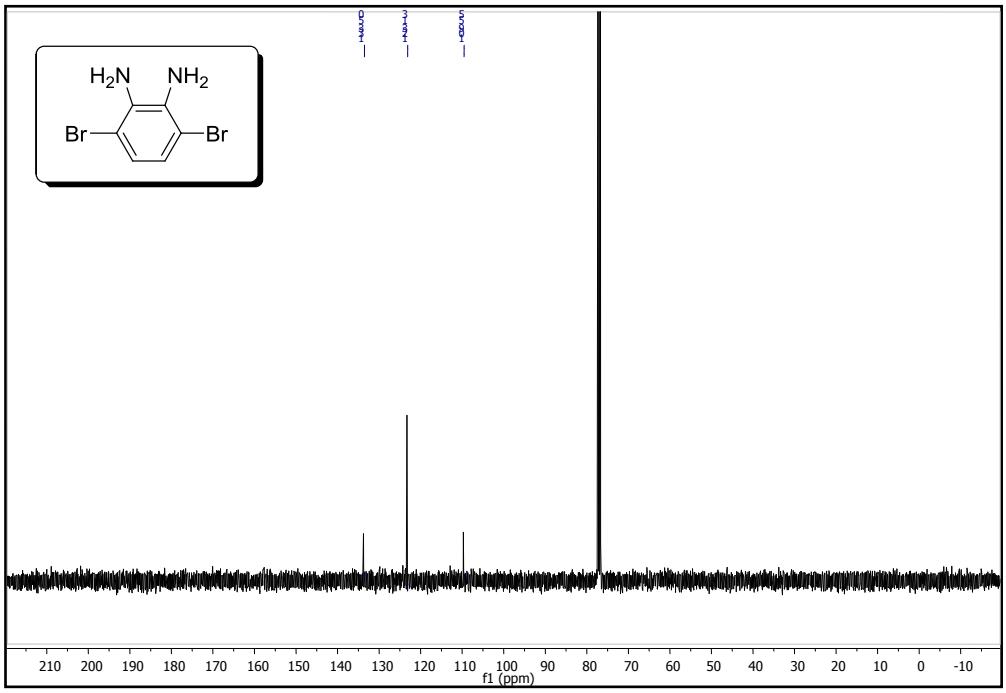

Figure A. 4 ^{13}C-NMR spectrum of 3,6-dibromobenzene-1,2-diamine (**3**)

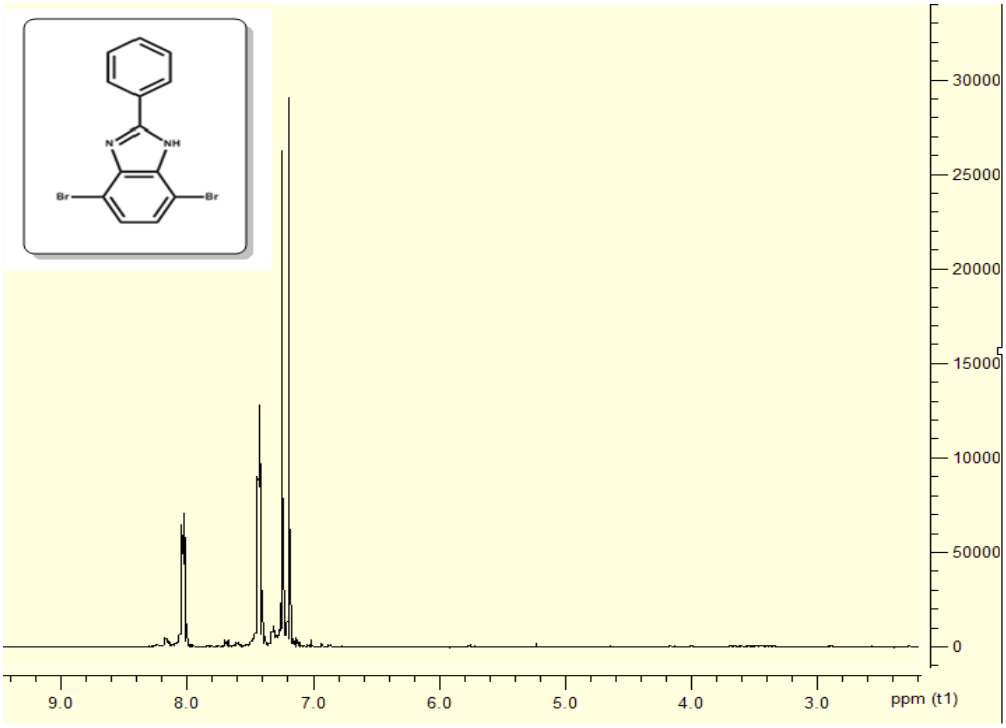

Figure A. 5 ^{1}H-NMR spectrum of 4,7-dibromo-2-phenyl-1H benzo[d]imidazole (**3a**)

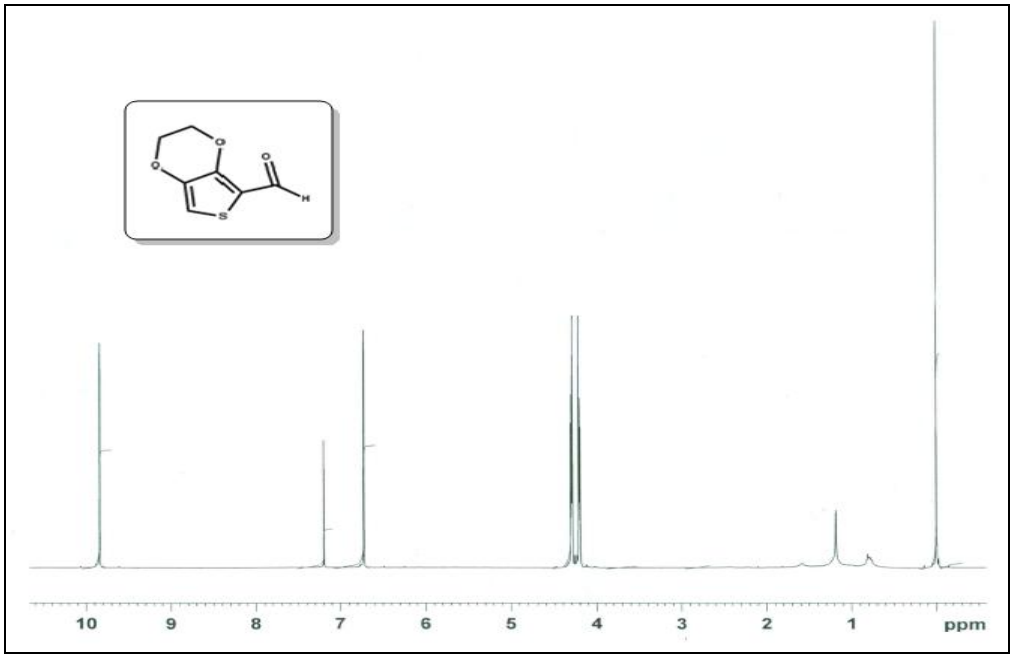

Figure A. 6 ^{1}H-NMR spectrum of 2,3-dihydrothieno[3,4 b][1,4]dioxine-5-carbaldehyde (**5**)

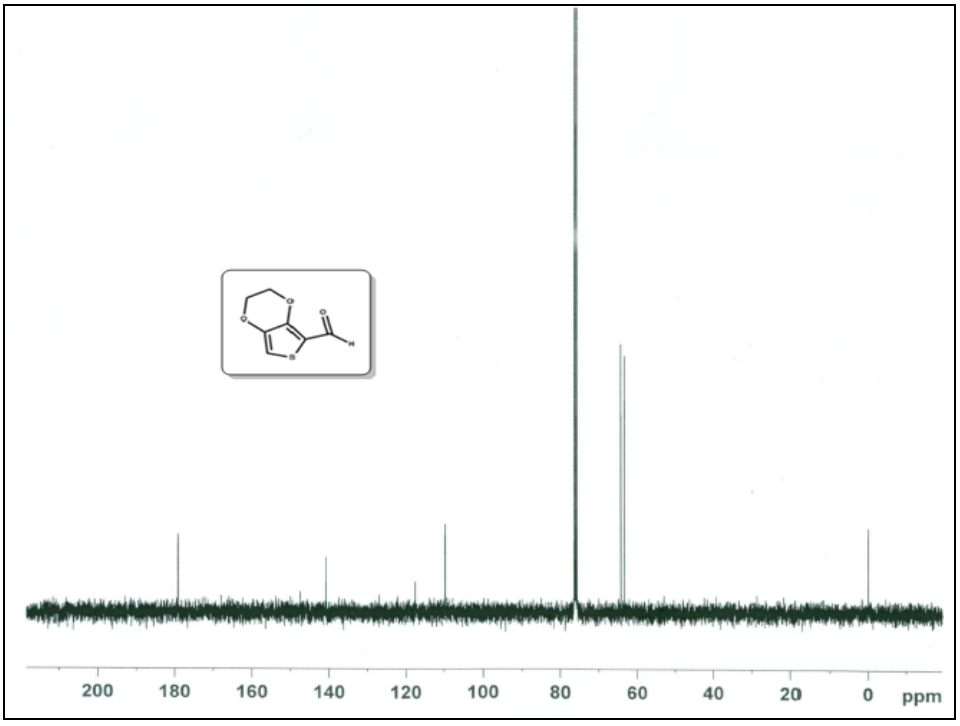

Figure A. 7 ^{13}C-NMR spectrum of spectrum of 2,3-dihydrothieno[3,4 b][1,4]dioxine-5-carbaldehyde (**5**)

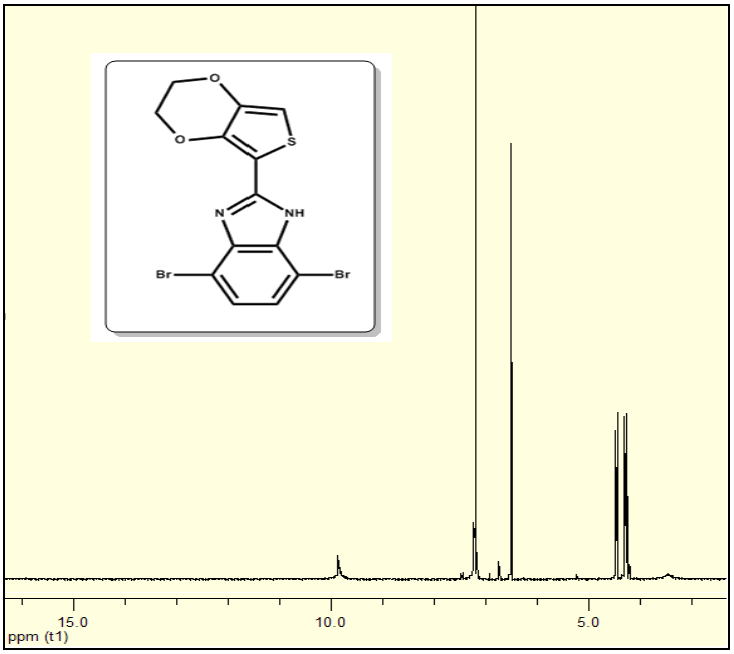

Figure A. 8 ^{1}H-NMR spectrum of 4,7- dibromo-2-(2,3-dihydrothieno[3,4-b][1,4]dioxin-5-yl)-1H-benzo [d]imidazole (**3b**)

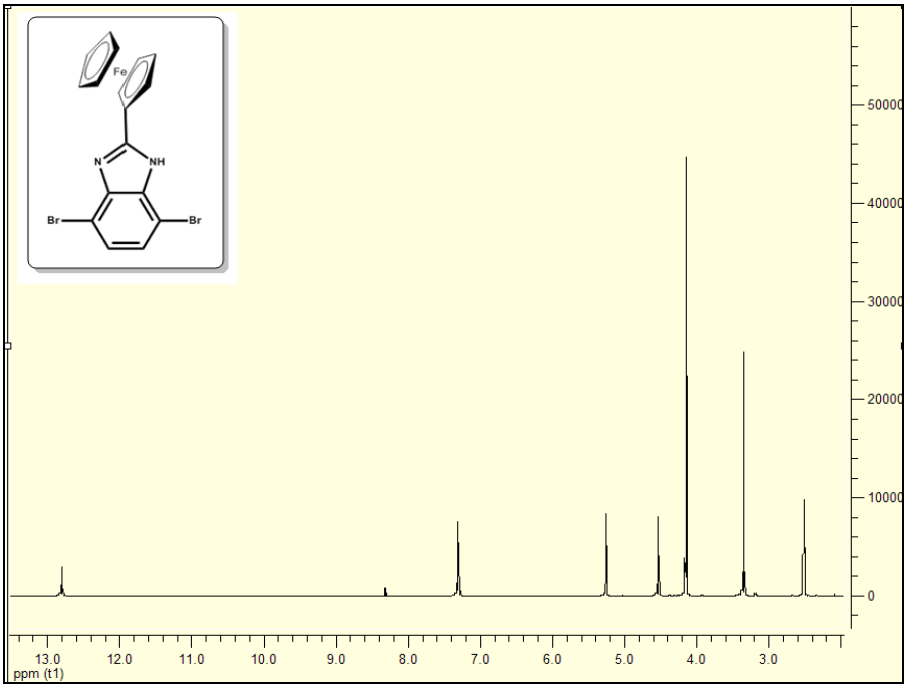

Figure A. 9 ^{1}H-NMR spectrum of 4,7-Dibromo-2-ferrocenyl-1H-benzo[d]imidazole (**3c**) (400 MHz, DMSO-d6, d).

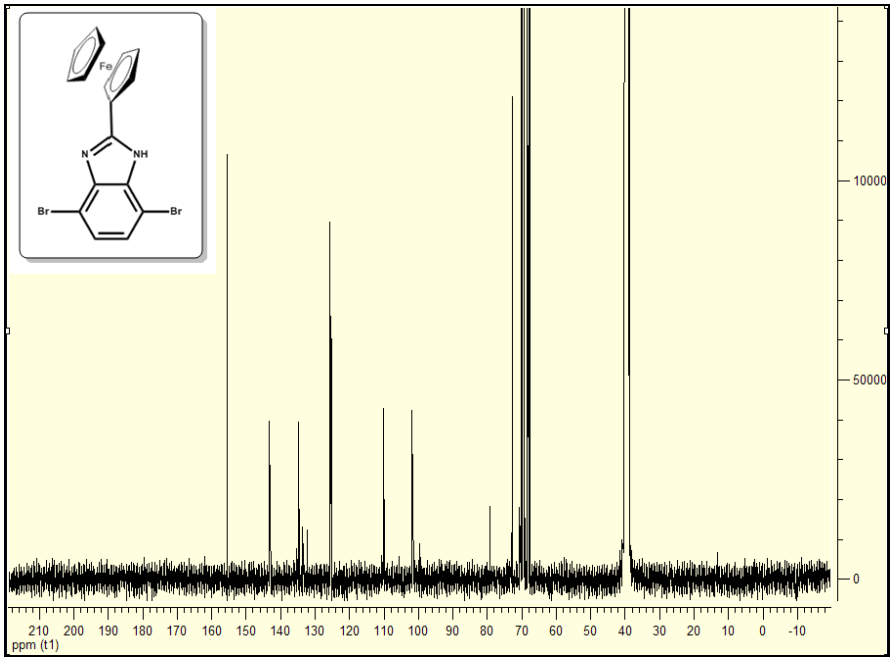

Figure A. 10 ^{13}C-NMR spectrum of 4,7-Dibromo-2-ferrocenyl-1H-benzo[d]imidazole (**3c**) (100 MHz, DMSO-d6, d).

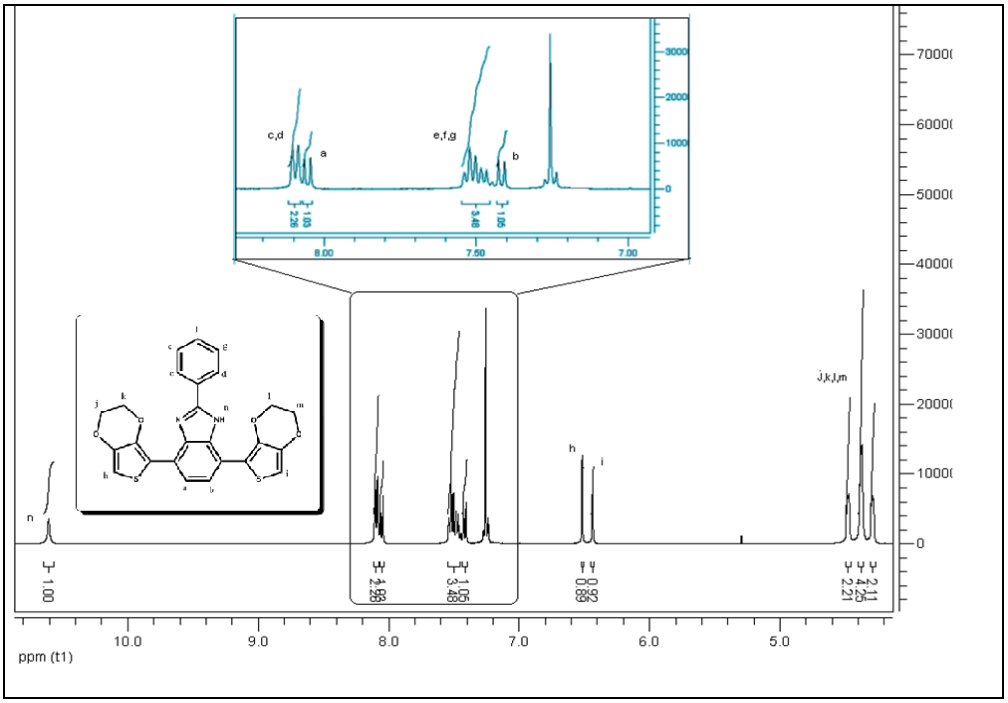

Figure A. 11 ^{1}H-NMR 4-(2,3-Dihydrothieno[3,4-b][1,4]dioxin-5-yl)-7-(2,3 dihydrothieno[3,4b][1,4] dioxin-7-yl)-2-benzyl-1H-benzo[d]imidazole (**M1**).

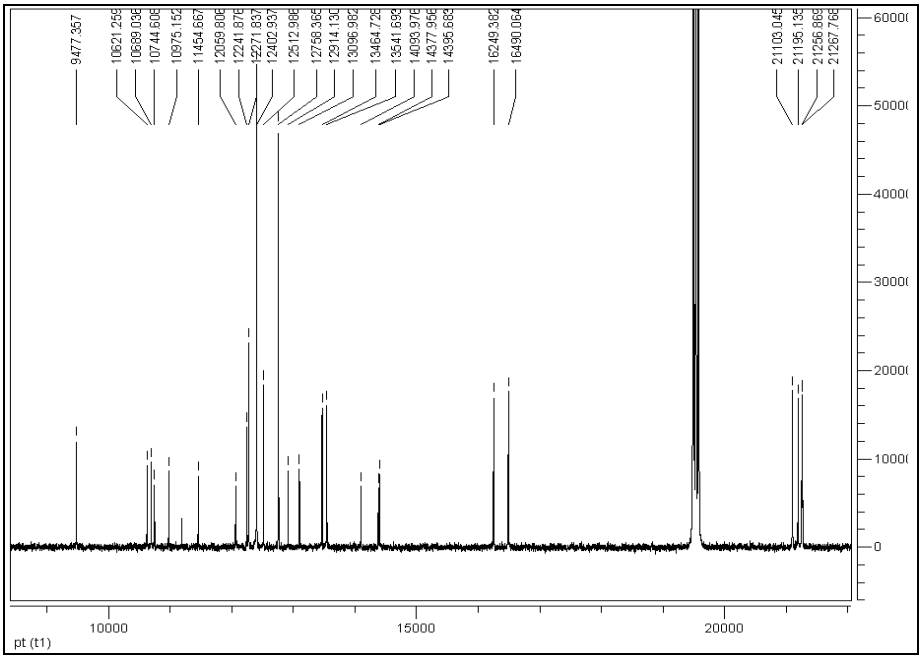

Figure A. 12 ^{13}C-NMR spectrum of 4-(2,3-Dihydrothieno[3,4-b][1,4]dioxin-5-yl)-7-(2,3 dihydrothieno[3,4b][1,4] dioxin-7-yl)-2-benzyl-1H-benzo[d]imidazole (**M1**).

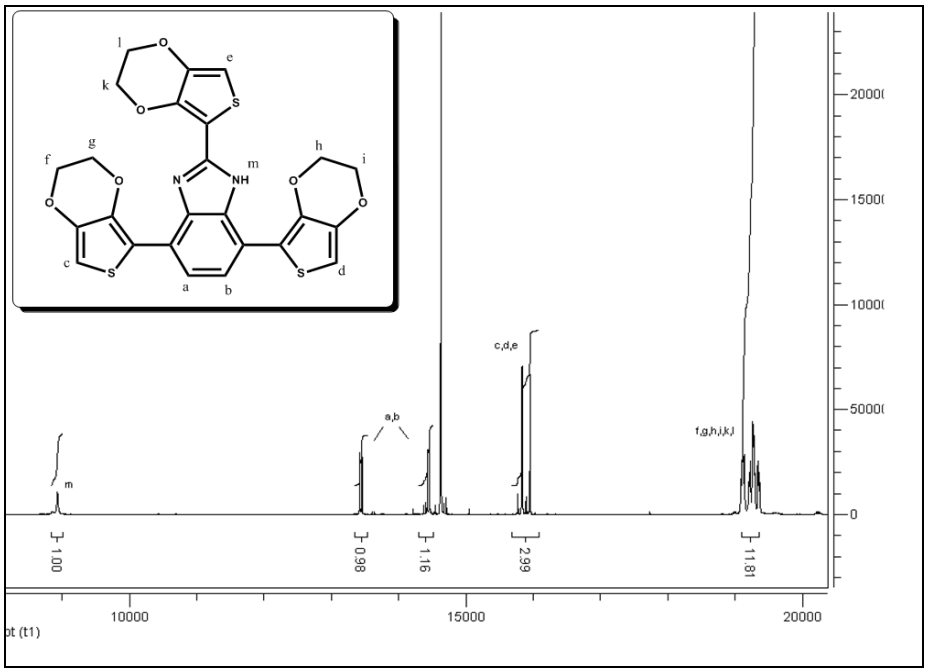

Figure A. 13 ^{1}H-NMR spectrum of 2,4-bis(2,3-dihydrothieno[3,4-b][1,4]dioxin-5-yl)-7-(2,3-dihydrothieno[3,4-b][1,4]dioxin-7-yl)-1H-benzo[d]imidazole (**M2**).

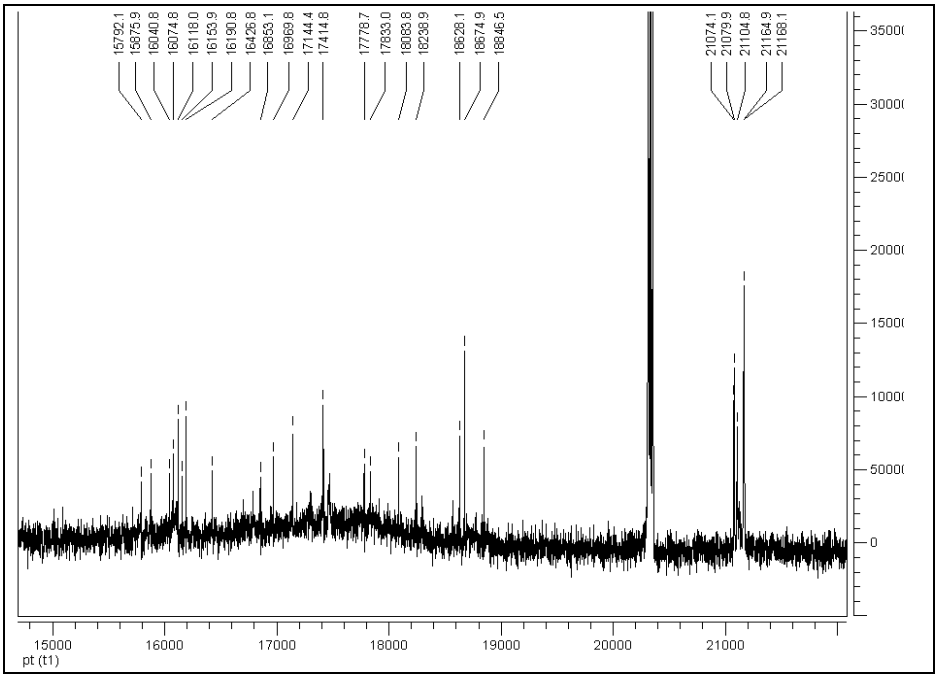

Figure A. 14 ^{13}C-NMR spectrum of 2,4-bis(2,3-dihydrothieno[3,4-b][1,4]dioxin-5-yl)-7-(2,3-dihydrothieno[3,4-b][1,4]dioxin-7-yl)-1H-benzo[d]imidazole (**M2**).

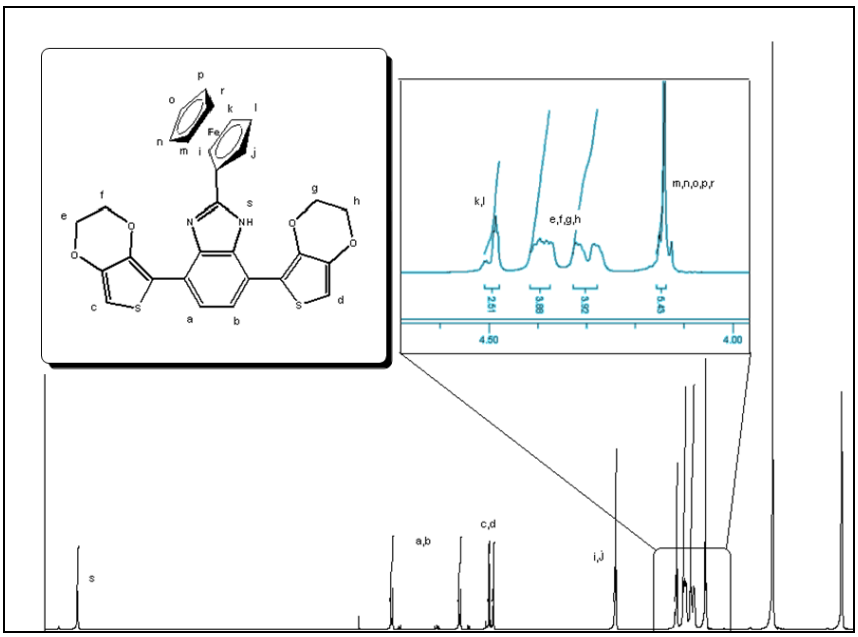

Figure A. 15 ^{1}H-NMR spectrum of 4-(2,3-dihydrothieno[3,4-b][1,4]dioxin-5-yl)-7-(2,3-dihydrothieno[3,4-b][1,4]dioxin-7-yl)-2-ferrocenyl-1H-benzo[d]imidazole (**M**3).

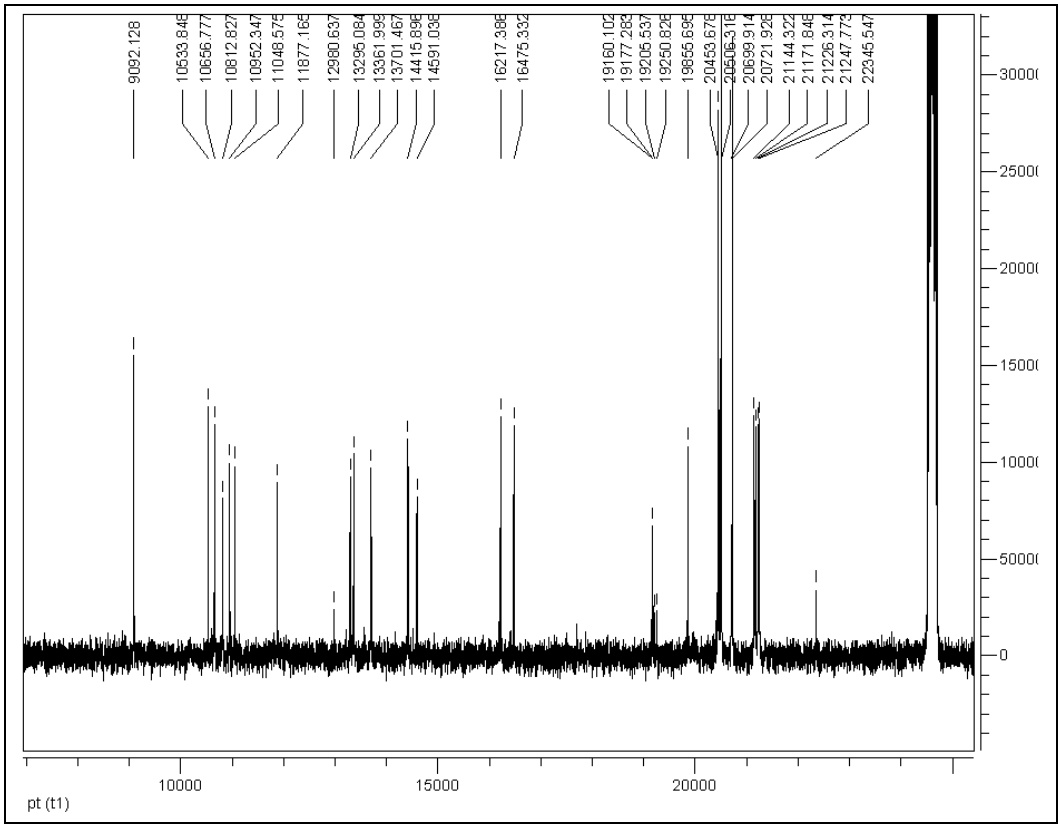

Figure A. 16 ^{13}C-NMR spectrum of 4-(2,3-dihydrothieno[3,4-b][1,4]dioxin-5-yl)-7-(2,3-dihydrothieno[3,4-b][1,4]dioxin-7-yl)-2-ferrocenyl-1H-benzo[d]imidazole (**M3**).